The role of wall layers properties on the thermal performance of ventilated facades: Experimental investigation on narrow-cavity design

Manuscript Details

Manuscript number	ENB_2019_2310_R1
Title	The role of wall layers properties on the thermal performance of ventilated facades: experimental investigation on narrow-cavity design
Article type	Full Length Article

Abstract

In this paper, we have investigated how different materials and thermal masses impact on the performance of ventilated facades with narrow cavities, by measuring the variation in terms of heat flows and ventilation efficiency. While geometry has been widely explored, the role of wall composition has received much less attention. To bridge the gap, three real-scale prototypes of ventilated facades were built and tested all over the year on a mock-up in Central Italy: (i) L, with a lightweight external enclosure, as a baseline reference, (ii) IM, with a massive layer enclosed in the gap and (iii) EM, with an external massive cladding. The results demonstrated that the EM solution more effectively mitigated the average surface temperatures (both external and internal), with values of –2°C and -1°C in summer and of -3°C and -0.5°C in winter, when compared to the L solution. Moreover, in the EM case, the ventilated cavity reduced both the incoming and outgoing heat fluxes, since the outer mass operated as a thermal buffer between the outdoor and the ventilation chamber. Conversely, the presence of an internal mass determined an increase of the heat transfer towards the indoor environment. The position of the thermal mass in the outer layer also increased the air velocity in the gap thus enhancing the stack effect.

Keywords	Ventilated facades; Experimental study; Thermal inertia; Energy efficiency; Narrow cavity;
Taxonomy	Architectural Engineering, Passive Design, Heat Transfer
Manuscript category	Passive and Natural Energy and Environmental systems and technologies

Corresponding Author	Francesca Stazi
Corresponding Author's Institution	Polytechnic University of Marche
Order of Authors	Francesca Stazi, Giulia Ulpiani, Marianna Pergolini, Costanzo Di Perna, marco d'orazio

Suggested reviewers	Maria Ibañez, Marina Vidaurre-Arbizu

Submission Files Included in this PDF

File Name [File Type]

Cover letter.docx [Cover Letter]

Letter to Reviewers.docx [Response to Reviewers]

F Stazi marked revised manuscript.docx [Revised Manuscript with Changes Marked]

Highlights.docx [Highlights]

F Stazi_unmarked revised manuscript.docx [Manuscript File]

01.tif [Figure]

02.tif [Figure]

03.tif [Figure]

04.tif [Figure]

05.tif [Figure]

06.tif [Figure]

07.tif [Figure]

08.tif [Figure]

09.tif [Figure]

10.tif [Figure]

Tables.docx [Table]

Conflict of Interest .docx [Conflict of Interest]

Author statement.docx [Author Statement]

To view all the submission files, including those not included in the PDF, click on the manuscript title on your EVISE Homepage, then click 'Download zip file'.

Research Data Related to this Submission

There are no linked research data sets for this submission. The following reason is given:
Data will be made available on request

Cover letter

7 August, 2019

Department of Materials, Environmental Sciences and Urban Planning (SIMAU)
Polytechnic University of Marche,
Via Brecce Bianche, 60131, Ancona, Italy.

Dear Editorial Board of Energy and Buildings,

The present submission regards a manuscript entitled “The role of wall layers properties on the thermal performance of ventilated facades: experimental investigation on narrow-cavity design” to be considered for publication as a research article in your journal.

The contents are novel and original. All authors have seen and approved the manuscript and have contributed significantly.

This research aims at experimentally evaluating the impact of different boundary conditions on the year-round behavior of narrow cavities in ventilated facades. It was demonstrated that the ventilated façade with a thermal mass adjacent to the outer side of the cavity (EM) exhibited an enhanced stack effect and reduced incoming and outgoing thermal fluxes, since the mass operated as a thermal buffer between the outdoor and the ventilation chamber.

Thank you very much for your consideration.

Kind regards,

Prof. Francesca Stazi, Corresponding Author
Polytechnic University of Marche
Via Brecce Bianche, 60131, Ancona, Italy.

Tel.: + 39 071 2204783

E-mail: f.stazi@univpm.it

Letter to Reviewers

Dear Editors and Reviewers,

Thank you for your comments concerning our manuscript entitled “The role of wall layers properties on the thermal performance of ventilated facades: experimental investigation on narrow-cavity design”.

By addressing each of the raised points, we trust the manuscript has much improved. The main corrections are marked in red within the paper and the responses to the reviewers’ comments are the following:

Reviewer 1

There are some references noticed at the end of the paper that do not appear in the paper such as references [1], [2], [3], [4] and [7]. They need to be marked in the paper.

The references have been inserted correctly in the paper.

Reviewer 2

The paper is well written, and shows original results based on the experimental assessment of three typologies of ventilated walls. The scope of the paper is within the topics of the journal and it is worth to be published. There are just minor changes to be made before the paper will be ready to be published.

The comments are the following:

- Despite indicating at page 4 that, for the location that has been considered, the hottest month is August and the coldest one is January, then the summer and winter performance are assessed respectively in September and December. The authors should better clarify the criteria used in the selection of the summer and winter monitoring period. On the same topic, the paper should better express why 5 consecutive days have been considered and not for example 10 or 15.

The climate in Agugliano is characterized by a summer average temperature ranging from 20°C (June and September) to 23°C (July and August), as seen in Fig.1. We used data collected in September since, as demonstrated elsewhere [1, 2], the thermal inertia benefits are better appreciated in periods characterized by cooler nights, since the mass is able to cool itself properly. Indeed, we noticed that the differences between the three experimented walls were more significant in September.

Only five days were reported, since it was the longest period with homogenous data and without temporary probe failures. Over this observation window it was possible to better control the validated data and to clearly identify a consistent trend.

Reference:

[1] F. Stazi, “Thermal Inertia in Energy Efficient Building Envelopes”, Butterworth-Heinemann 2017.

[2] F.Stazi, G. Ulpiani, M. Pergolini, C. Di Perna, “The role of areal heat capacity and decrement factor in case of hyper insulated buildings: an experimental study”, Energy Build., vol. 176, pp.310-324, 2018.

	January	February	March	April	May	June	July	August	September	October	November	December
Avg. Temperature (°C)	4.9	6.3	8.9	12.3	16.5	20.4	23	23	19.8	15.3	10.7	6.7
Min. Temperature (°C)	2.1	3.3	5.4	8.5	12.5	16.3	18.8	18.9	16	11.9	7.8	3.9
Max. Temperature (°C)	7.7	9.4	12.4	16.2	20.6	24.6	27.3	27.1	23.6	18.7	13.7	9.5
Avg. Temperature (°F)	40.8	43.3	48.0	54.1	61.7	68.7	73.4	73.4	67.6	59.5	51.3	44.1
Min. Temperature (°F)	35.8	37.9	41.7	47.3	54.5	61.3	65.8	66.0	60.8	53.4	46.0	39.0
Max. Temperature (°F)	45.9	48.9	54.3	61.2	69.1	76.3	81.1	80.8	74.5	65.7	56.7	49.1
Precipitation / Rainfall (mm)	59	53	63	61	61	55	50	66	75	74	82	73

Fig. 1. Average external temperature in Agugliano (from https://en.climate-data.org/europe/italy/marche/agugliano-116114/)

With regard to wintertime, either January or December can be the coldest month in Agugliano: for instance, in 2018, the average temperature was 6.7 °C in December and 8.1°C in January, while in 2017, the corresponding temperatures were 7.2°C and 4°C, according to the relevant weather archive of the closest (10 km) weather station (https://www.ilmeteo.it/portale/archivio-meteo/Ancona/2018/Agosto). Therefore both months are suitable for a representative analysis of winter conditions.

- The test room seems not to be properly representative of a typical construction for the climate zone considered in the paper. The walls seem to be hyperinsulated (U-value of less than an half of the maximum required one) and also there is absence of internal gains or solar gains. The authors, in the final discussion, should better argue on the selection of the test room, of its representativeness

for the conditions of application of the technologies studied and on the replicability and generalization of the results.

Even in mild climates as Mediterranean's, the construction sector is moving towards higher and higher insulation levels, thus decoupling the behavior of the internal environment from the external one and ascribing this relationship to the windows rather than to the opaque wall. As a consequence, we have adopted a hyper-insulated envelope and have focused exclusively on the outer side of the opaque wall to gain insight into the behavior of the cavity only with respect to its adjacent layers, facing outwards.

Indeed, the main purpose of the study was identifying the impacts of different materials adjacent to the air cavity, regardless of the internal layers, also to expand the applicability of the results.

To clarify the reasons of this choice, also to the readers, the authors have added this explanation also in the discussion section of the manuscript.

Title page

The role of wall layers properties on the thermal performance of ventilated facades: experimental investigation on narrow-cavity design

First author and corresponding author

Francesca Stazi [(a)]

E-mail: f.stazi@univpm.it

Tel: (+39) 3283098217

Second author

Giulia Ulpiani [(b)]

E-mail: g.ulpiani@pm.univpm.it

Third author

Marianna Pergolini [(a)]

E-mail: m.pergolini@hotmail.it

Fourth author

Costanzo Di Perna [(b)]

E-mail: c.diperna@univpm.it

Fifth author

Marco D'Orazio [(c)]

E-mail: m.dorazio@univpm.it

Affiliation

(a) Department of Materials, Environmental Sciences and Urban Planning (SIMAU), Polytechnic University of Marche, Ancona, Italy

(b) Department of Industrial Engineering and Mathematical Sciences (DIISM), Polytechnic University of Marche, Ancona, Italy

(c) Department of Civil, Constructional and Environmental Engineering (DICEA), Polytechnic University of Marche, Ancona, Italy

The role of wall layers properties on the thermal performance of ventilated facades: experimental investigation on narrow-cavity design

F. Stazi[(a)], G. Ulpiani[(b)], M. Pergolini[(a)], C. Di Perna[(b)] , M. D'Orazio [(c)]

(a) Department of Materials, Environmental Sciences and Urban Planning (SIMAU), Polytechnic University of Marche, Ancona, Italy

(b) Department of Industrial Engineering and Mathematical Sciences (DIISM), Polytechnic University of Marche, Ancona, Italy

(c) Department of Civil, Constructional and Environmental Engineering (DICEA), Polytechnic University of Marche, Ancona, Italy

Abstract

In this paper we have investigated how different materials and thermal masses impact on the performance of ventilated facades with narrow cavities, by measuring the variation in terms of heat flows and ventilation efficiency. While geometry has been widely explored, the role of wall composition has received much less attention. To bridge the gap, three real-scale prototypes of ventilated facades were built and tested all over the year on a mock-up in Central Italy: (i) L, with a lightweight external enclosure, as a baseline reference, (ii) IM, with a massive layer enclosed in the gap and (iii) EM, with an external massive cladding. The results demonstrated that the EM solution more effectively mitigated the average surface temperatures (both external and internal), with values of –2°C and -1°C in summer and of -3°C and -0.5°C in winter, when compared to the L solution. Moreover, in the EM case, the ventilated cavity reduced both the incoming and outgoing heat fluxes, since the outer mass operated as a thermal buffer between the outdoor and the ventilation chamber. Conversely, the presence of an internal mass determined an increase of the heat transfer towards the indoor environment. The position of the thermal mass in the outer layer also increased the air velocity in the gap thus enhancing the stack effect.

Keywords: Ventilated facades, Experimental study, Thermal inertia, Energy efficiency, Narrow cavity.

1. Introduction

In the roadmap for a constant pursuit of durability improvement of buildings outer surfaces, Ventilated Skins (VS) were originally conceived as rain screens, finding application in both retrofitting and new buildings interventions. International studies demonstrated that they could also be effective as a passive cooling strategy on annual basis, with respect to the unventilated option [1-9].

The ventilated skin is an external coating system, secured to the building envelope by means of mechanical anchoring points. It consists of four functional layers (from the inner side to the outer side): (i) internal layer; (ii) continuous insulation layer; (iii) ventilation chamber with lower and upper openings connected to the outdoor air; (iv) external cladding [10, 11]. Many parameters influence the air gap behavior and, ultimately, the impacts on the building energy budget. They can be divided in two main categories:

- outdoor boundary conditions, such as geographical localization [12], solar radiation [13] and wind speed [14];
- design choices, namely width and height of the ventilation gap [15], external cladding material [16,17] and joints configuration that can be either open [18] or closed [19]. These research studies focused on the evaluation of one single facade typology, but no study concerned the simultaneous comparison between walls with different external VS solutions.

The ventilated skin is an efficient system for both summer and winter. In the summertime, the thermal gradient between upper and lower openings activates the air flow (driven by buoyancy and wind forces) allowing the heated air in the ventilation chamber to be expelled through the outlet opening, hence reducing the heat gains toward the indoors [6, 10, 12, 14, 20]. In the wintertime, the ventilation gap behaves as a thermal buffer that accumulates heat and dampens the temperature difference between inside and outside, thus curbing transmission losses. Moreover, it positively affects the thermal resistance of the wall. This aspect was rarely investigated in existing studies [21, 22].

The key purpose of the present experimental research was to determine the impact of different materials adjacent to the air cavity on the heat fluxes and ventilation efficacy. Three prototypes were experimentally tested, simultaneously: one lightweight with plastered OSB panel (hereafter termed “L”), one with internal mass and the same external lightweight OSB panel (“IM”) and one with external massive cladding through the use of hollow bricks (“EM”). Extensive measurements were collected and analyzed to compare the thermo-physical performance and natural ventilation potential, with respect to the buoyancy and wind forces. For each prototype, the following parameters were measured: the surface temperature on the outer side of the façade and on the inner side of the gap, the heat fluxes, the air speed and the temperature in the gap.

2. Experimental method

2.1 Ventilated Skin prototypes

The experiment was carried out in Agugliano, Central Italy, featuring Csa climatic conditions according to the K□ppen-Geiger classification: the hottest month is August (average temperature around 32°C) and the coldest one is January (average temperature around 8°C).

The skins were mounted on the western façade of an experimental mock-up (Fig. 1a), exposed to direct sunlight over the hottest afternoon hours and thus being more susceptible to overheating [23].

The mock-up is representative of a full-scale, single rectangular room (net area of 12.2 m^2). The load bearing structure is made of cross laminated timber panels. The building is highly insulated, with insulation layers placed both on the external and the internal sides. Also, it is unoccupied and windowless to avoid unequal contributions of the solar radiation and uncontrollable internal heat gains. The wall composition is detailed in Table 1 (see layers 1-6). The thermal transmittance, measured *in-situ* according to the Standard ISO 9869 [24], is 0.13 W/m^2K.

The west-facing wall of the mock-up covers 9 m^2 (3.22 m length x 2.80 m height). Three rectangular-shaped ventilated skins were tailor-made to fit in the available surface (Fig.1b), with each modulus of 1 m length x 2.30 m height, raised 30 cm off the ground.

As specified in Table 1, the L configuration featured an aerated gap (layer 7) enclosed by a white plastered, oriented strand board (OSB) (layers 8-9) and it was used as reference for comparisons. The IM configuration had a massive layer (7) in between the insulation material and the air gap, while the EM configuration exhibited the massive layer (8) on the outer side of the air gap, finished with white plaster (9).

For all the facades, a narrow cavity was selected (0.06 m width) to emphasize the contribution of different materials enclosing the gap. Moreover, this value is intermediate among the most common [11] and it is the most suitable solution for the selected metallic substructure.

The white plaster was intentionally adopted for the three outer skins as to prevent any bias due to different optical properties. The emissivity was 0.9 and the solar reflectance was 0.60. The thermo-physical properties of the abovementioned materials, given by the manufactures, are presented in Table 2 while Fig. 2 shows the cross section of the three prototypes.

The facades were assembled using vertical wooden batten support frames, and bottom steel supporting brackets screwed to the cross laminated timber structure, coupled with thermal cutting plates to eliminate thermal bridges (Fig. 2, insert A). XPS insulation layers were sealed on either side of each wall to enclose the air chambers. Honey-combed nets were placed to protect the cavities.

Standards EN ISO 6946:2008 and EN ISO 13786:2008 were adopted for the characterization of the thermal parameters of the three ventilated modules, considering a well ventilated air chamber (Table 3). L and EM enclosures show equal thermal features, given that the calculation disregards the thermal resistance of the air layer and all the other layers between the air gap and the external environment. Table 3 also reports the values of the external areal heat capacity $\boldsymbol{k}_2$ (obtained according to the same standards) but including all the layers in the calculation. In this case, the three prototypes showed increasing levels of inertia, from the lowest value of L (28 kJ/m^{2}K) to the highest one of EM (60 kJ/m^{2}K).

External and internal surface temperatures and heat fluxes data were analyzed by means of the following statistic distribution measures in order to avoid outliers:

- 99th percentile to indicate the maximum value;
- The median (Q2) to indicate the middle value;
- The interquartile range (IQR) as the difference between the upper (Q3) and lower (Q1) quartiles to describe the values spread.

2.2 Sensors network

The monitoring activity was carried out throughout the year in order to examine the thermal behavior of the ventilated skins during different seasons. A set of devices was installed to record:

1. Outdoor temperature, relative humidity, global solar radiation, speed and direction of the wind. Data were collected using a weather station, 3 m away from the ventilated facades;
2. Surface temperatures of the outermost and innermost layers at the bottom (60 cm), middle (115 cm) and top (168 cm) of each façade. Thermo-resistance sensors (accuracy ± 0,05 °C) were adopted;
3. Incoming and outgoing heat fluxes at mid-height (115 cm) in the innermost side of the air chamber, measured by heat flux plates (accuracy ± 3%);
4. Air velocity and air temperature inside the ventilation chamber at mid-height (115 cm). Data were collected using TESTO hot-sphere anemometers (accuracy ±0.03 m/s).

The output analog signals from the probes were digitized by means of NI-DAQ acquisition modules. LabVIEW was used to manage the dataflow and its elaboration. The acquisition rate was 5 minutes. The sensor network was arranged as displayed in Fig. 3.

3. Summer results

This paragraph shows the results from the experimental campaign in summertime. Fig. 4 provides an overview of the weather conditions of 5 consecutive days, representative of the typical Mediterranean summer climate.

3.1 Surface temperature and fluxes

The external surface temperatures profiles are plotted in Fig. 5a. We used data collected in September since, as demonstrated elsewhere [22, 25], the thermal inertia benefits are better appreciated in periods characterized by cooler nights, since the mass is able to cool itself properly. Indeed, we noticed that the differences between the three experimented walls were more significant in September. As expected, the values recorded at 115 cm were always significantly higher than the ambient air. Moreover, when the sun hit the western façade in the afternoon (14:00 – 18:00), the values notably increased, with an average offset of 7°C. EM showed daily peaks almost 2°C lower than the other two configurations over the hottest hours (see September 12th). All the surface temperatures plummeted overnight. The EM solution touched the absolute minima since the outer mass released the stored heat outwards, without showing any conservative behavior.

Fig. 5b reports the surface temperatures measured on the innermost side of the cavity at mid-height (115 cm). L experienced the greatest thermal range, reaching daytime maxima (exceeding the ones of the outdoor air when the sun hit the façade) and the minima by night (very close to the outdoor air). By contrast, EM and IM showed milder fluctuations. EM registered the lower values throughout the day since it dissipated, in a more effective way, the retained heat. These observations got confirmed by the statistical analysis in Table 4, that shows how EM guaranteed temperature reductions of about 4.7% on the external surface and of 7.2% on the internal one, compared to L.

The thermal flux trends for the three walls (recorded at mid-height, on the inner side of the air gap), are shown in Fig. 5c. The heat fluxes are positive with an incoming direction towards the test room. Around peak hours (11:00 – 16:00), the IM prototype flux reached the highest values, compared to those recorded by the other two. This might be explained by considering that, for this wall only, the heat flux plate measured the storing action, since it was placed directly on the hollow bricks. In contrast, the EM heat flux was negligible in the morning and increased only later in the afternoon (with an inward direction). The mass positioned on the external side of the air gap operated as a thermal buffer between the outdoors and the ventilation chamber, strongly mitigating the driving force for heat transmission.

Therefore, it required more time before an appreciable thermal gradient could be spotted on the edge of the air gap, triggering the heat flow. In the evening, the heat flow reversed (negative sign). In particular, heat fluxes of IM and L suddenly dropped with very similar slopes while EM underwent a milder decline because of the external mass inertial storing action. The reduction of the heat coming from the outside between EM and IM approached 70 % (Table 4).

3.2 Wind action and stack effect in summer

EM and IM were compared in terms of airflow rate in two summer days (Fig.6), namely September 8th and 12th, characterized by similar daily average solar radiation (around 400 W/m^2) but different wind speeds (averages of 2.3 m/s and 1.4 m/s, respectively), coming from the same prevalent direction for the selected site (North).

The air speed profiles in the gaps followed the wind trends: the stack effect was accentuated in the windiest day for both configurations with a 30% velocity bump with respect to the unventilated day (Fig.6). Consequently, the temperatures of the internal surface and the air within both the cavities diminished.

However, unequal wind speed values did not alter significantly the distance among the temperature curves characterizing the two walls. The EM internal surface temperature curve was always lower than the other, except in the morning hours (10:00-15:00 time slot), and it reached the highest maximum peak between 15:00 and 18:00. Furthermore, the air temperatures in the gaps almost coincided, until 15:00. IM showed greater fluctuations, reaching the highest maximum value and descending with a more tilted trend.

4. Winter results

The present section illustrates the results obtained from the winter monitoring campaign. A representative set of the outdoor boundary conditions in the coldest months is showed in Fig. 7.

4.1 Surface temperature and fluxes

The winter temperature trends of the external surfaces, recorded at mid height (115 cm), are presented in Fig. 8a. All the temperatures were higher than the outdoor air in the middle of the day. L reached again the highest values, with peaks approximately 1°C above IM. The EM external surface temperature remained the coolest throughout the day lowering the daily peaks down to 5°C on the warmest day (December 26th) with respect to the others. During the nighttime, the outer surface temperatures of the three walls dropped significantly. As in summertime, EM stayed around 2°C cooler than the other configurations since the outer mass could completely cool itself. In the morning hours, this led to a significant difference (around 3°C) between the rising outdoor temperature and EM surface temperature.

Fig.8b reports the surface temperatures on the innermost side of the gap. The curves confirmed the summer trends, with less pronounced fluctuations for the massive walls and more emphasized for the lightweight solution. As demonstrated by the statistical analysis in Table 5, the surface temperature reduction between L and EM is more noticeable than in summer, touching –20% and -27% for the external and internal surface temperatures, respectively.

The daily heat flux trends were very similar to those recorded in summertime (Fig. 8c) with EM always recording the minima.

4.2 Wind action and stack effect in winter

The airflow rates of EM and IM were compared on two different days (Fig.9), namely December 25th and 27th, characterized by similar daily average solar radiation (200 W/m^2) but different wind speeds (average values of 2 m/s and 1 m/s, respectively), again in the north direction.

The same observations made in 3.2 could be drawn also for the winter season (Fig. 9). Even in winter, the air speed trends in the gaps followed the wind fluctuations and, as expected, the stack effect was more pronounced in the windiest day for both the massive configurations. The mean air speeds within the cavity were 0.17-0.22 m/s for EM and 0.11-0.20 m/s for IM. As the wind force was halved, also the average air velocities in the gap of both walls experienced a reduction of nearly 50%. The air speed in the ventilation gap was negligible at night while it reached the highest values over peak hours. Nonetheless, the relative behavior between the two walls was maintained. The EM internal surface temperature stayed always higher than the other one, notably during the afternoon hours. Conversely, the air temperatures within the gaps had almost the same trends.

5. Discussion

The present work deals with the effect of adopting different materials in the boundaries of the ventilated gap, in the case of narrow cavities, in summer and winter. It was experimentally demonstrated that the use of massive layers is beneficial in terms of temperature reduction: both prototypes with high mass within the cavity (EM and IM) exhibited reduced internal surface temperatures in the inner side of the gap and lower air gap temperatures, with respect to the solution with lightweight materials (L). Moreover, the mass should be preferably positioned on the outer side of the cavity (EM) guaranteeing lower incoming/outgoing fluxes and higher stack effect with respect the internal mass solution (IM).

This result is novel in literature, yet well in accordance with previous researches. Indeed, while the most common studies vary the type of the external cladding (e.g. aluminum, terracotta, etc.) and the thermal resistance of the

internal layers, more rare are the researches that address the effect of the change of the mass position with respect to the cavity (internal or external side).

The change of the external cladding (e.g. stone cladding rather than aluminum) has demonstrated to affect both the chimney effect efficacy and the long-wave thermal radiation within the air cavity as a result of the change of the radiative properties of the exterior finishing [26]. Other research that envisaged the comparison between alternative materials was carried out by Ciampi et al. [27]. In particular, changing only the external claddings from massive terra cotta to lightweight copper, they demonstrated that the former is the most convenient from the energy point of view. Some other authors, by comparing facades with very different layers stressed that the performance of the façade is influenced by the repartition of thermal resistance between the layers on the inner and outer sides of the cavity [28]. They introduced a dimensionless parameter *z*, representing the fraction of thermal resistance facing the external environment and demonstrated its correlation with the incoming heat fluxes through the ventilated façades and ventilation efficacy. The higher the parameter *z*, the more efficient the ventilation. For the prototypes of the present study, this parameter is about 9% for EM wall and around 3% for IM and L walls, thus confirming their findings.

The change of the thermal properties of the layer on the internal side of the cavity was instead addressed by Guillen et al. [29]. In particular, they analyzed the effect of the increase of the insulation level of the internal layers. This affected both the thermal periodic transmittance and the time lag but no mention was done on the effect of this change on the cavity performance. Another investigation in this topic was carried out by Prada et al. [30]. They compared two cases, one with insulation behind the cavity and one considering a not insulated mass. Moreover, they changed the emissivity of the cavity inner surface to deepen its effect on the air motion and heat transfer. They highlighted that the insulated wall reached higher air velocities for the entire wall height. This result is also confirmed by our data (see table in Fig.10) regarding winter and summer air velocities in the cavities for all the three prototypes. The L solution, even if characterized by high summer temperatures and winter crossing fluxes, exhibits a good stack effect all year round.

The abovementioned studies are commonly based on analytical comparisons and mainly aimed at highlighting the effect of different cavity geometries. Moreover, at the author's knowledge, no studies focused on the comparison of alternative configurations using the same materials and under the same optical properties for the external finishing but modifying the mass position. The present research aims at filling the highlighted gap through experimental data. This study is intentionally focused on narrow cavities since several authors demonstrated that the materials adjacent to a restricted gap have higher influence on its energy balance and ventilation efficacy [11].

Even in mild climates as Mediterranean's, the construction sector is moving towards higher and higher insulation levels, thus decoupling the behavior of the internal environment from the external one and ascribing this

relationship to the windows rather than to the opaque wall. As a consequence, we have adopted a hyper-insulated envelope and have focused exclusively on the outer side of the opaque wall to gain insight into the behavior of the cavity only with respect to its adjacent layers, facing outwards.

The results are synthetized and comparatively evaluated in Fig.10, that reports the hourly temperatures for a single summer (September 12th) and winter (December 24th) day, by superimposing the data to the walls sections. The temperature values recorded outdoors, in the outer surface, in the air cavity and in the innermost side of the gap are plotted during the central day hours for both seasons. Hourly values of air cavity velocity, global solar radiation and wind speed are also reported in the tables within the figure.

In the warmest season (Fig. 10a), the peak on the outer skin was recorded at 15:00 for all the facades, with L reaching the absolute maximum. Low air temperatures within the cavity are desirable to maximize the heat expulsion through the envelope [31]. This was the case of the massive configurations (EM and IM) that recorded almost the same temperature range (25°C-26.5°C), differently by L wall that reached values up to 28°C. Hence, the adoption of a thermal mass in contact with the air gap, irrespectively of the relative position, could be beneficial in terms of heat transfer reduction.

Even in the coldest season, EM recorded the lowest air cavity temperatures (Fig.10b). L reached higher surface temperatures only during the central hours of the day, peaking around midday, while in the evening it behaved similarly to the other two claddings. It could be concluded that the EM configuration recorded a more homogeneous behavior, both in summer and winter, with air temperatures in the gap and air speeds almost uniform throughout the day, and with the lowest internal surface temperatures in summer.

These results are obtained for the climate of Agugliano, characterized by a hot dry summer Mediterranean climate. In summer the average temperatures are about 23°C while in winter they drop down to 9°C. However, more detailed studies on the replicability of the results in other climatic contexts should be addressed.

6. Conclusion

The present experimental research was carried out with the purpose of establishing the impact of different boundary conditions on the year-round behavior of narrow cavities in ventilated facades. Three real-scale prototypes were designed and simultaneously monitored on a mock-up in Central Italy: one with a lightweight external cladding as reference (L), one with a massive layer in the innermost side of the air gap and a lightweight finishing (IM) and one with an outer massive enclosure (EM). Extensive measurements were conducted in summer and winter in order to identify the trends of the surface temperatures, the airflow rate in the gaps, and the heat fluxes.

It was experimentally demonstrated that the EM facade exhibited the coolest external and internal surface temperatures and the lowest incoming heat fluxes. The outer mass operated as a thermal buffer between the outdoors and the ventilation chamber hence reducing the incoming and outgoing heat fluxes through the envelope both in summer and winter. Moreover, the insertion of a thermal mass in the outer layer increased the air velocity in the gap hence emphasizing the stack effect. Also the internal mass IM was beneficial in terms of surface temperature, but it facilitated the heat transfer towards the indoor environment, thus incrementing summer gains.

Therefore, it was concluded that the adoption of a massive material in the outer side of a narrow gap (EM prototype) represented the optimal solution on annual basis, considering both the thermo-physical performance and the natural ventilation potential. Further investigation will address the potential for energy savings, also considering other materials and under condition of controlled air speeds.

Acknowledgements

The research was supported by HALFEN Company and by StilCasa Costruzioni. A particular thank to Eng. Andi Celaj, for the construction of the ventilated prototypes. The authors also want to express their gratitude to CENTROLEGNO and in particular to its CEO Roberto del Bianco, for the provision of the cross laminated timber test room.

REFERENCES

[1] C. Rosenzweig, W. D. Solecki, L. Parshall, M. Chopping, G. Pope, and R. Goldberg, “Characterizing the urban heat island in current and future climates in New Jersey,” *Environ. Hazards*, vol. 6, no. 1, pp. 51–62, 2005.

[2] M. Santamouris, “Regulating the damaged thermostat of the cities—Status, impacts and mitigation challenges,” *Energy Build.*, vol. 91, pp. 43–56, Mar. 2015.

[3] E. Di Giuseppe, M. Pergolini, and F. Stazi, “Numerical assessment of the impact of roof reflectivity and building envelope thermal transmittance on the UHI effect,” *Energy Procedia*, vol. 134, no. 2016, pp. 404–413, 2017.

[4] Y. Wang, U. Berardi, and H. Akbari, “Comparing the effects of urban heat island mitigation strategies for Toronto, Canada,” *Energy Build.*, vol. 114, pp. 2–19, 2016.

[5] M. Santamouris *et al.*, “On the energy impact of urban heat island in Sydney: Climate and energy potential of mitigation technologies,” *Energy Build.*, vol. 166, pp. 154–164, 2018.

[6] M. Santamouris, “Using cool pavements as a mitigation strategy to fight urban heat island - A review of the actual developments,” *Renew. Sustain. Energy Rev.*, vol. 26, pp. 224–240, 2013.

[7] P. Seferis, P. Strachan, A. Dimoudi, and A. Androutsopoulos, “Investigation of the performance of a ventilated wall,” *Energy Build.*, vol. 43, no. 9, pp. 2167–2178, 2011.

[8] M. Ciampi, F. Leccese, and G. Tuoni, “Cooling of buildings: Energy efficiency improvement through ventilated structures,” vol. 7, no. January 2003, pp. 199–210, 2003.

[9] M. Shahrestani *et al.*, “Experimental and numerical studies to assess the energy performance of naturally ventilated PV façade systems,” *Sol. Energy*, vol. 147, pp. 37–51, 2017.

[10] D. Bikas, K. Tsikaloudaki, K. J. Kontoleon, C. Giarma, S. Tsoka, and D. Tsirigoti, “ScienceDirect Ventilated Facades: Requirements and Specifications Across Europe,” *Procedia Environ. Sci.*, vol. 38, pp. 148–154, 2017.

[11] M. Ibañez-Puy, M. Vidaurre-Arbizu, J. A. Sacristán-Fernández, and C. Martín-Gómez, “Opaque Ventilated Façades: Thermal and energy performance review,” *Renew. Sustain. Energy Rev.*, vol. 79, no. May, pp. 180–191, 2017.

[12] F. Peci López and M. Ruiz de Adana Santiago, “Sensitivity study of an opaque ventilated façade in the winter season in different climate zones in Spain,” *Renew. Energy*, vol. 75, pp. 524–533, 2015.

[13] E. Iribar-Solaberrieta, C. Escudero-Revilla, M. Odriozola-Maritorena, A. Campos-Celador, and C. García-Gáfaro, “Energy performance of the opaque ventilated facade,” *Energy Procedia*, vol. 78, pp. 55–60, 2015.

[14] A. Gagliano, F. Nocera, and S. Aneli, “Thermodynamic analysis of ventilated façades under different wind conditions in summer period,” *Energy Build.*, vol. 122, pp. 131–139, 2016.

[15] C. Marinosci, G. Semprini, and G. L. Morini, “Experimental analysis of the summer thermal performances of a naturally ventilated rainscreen facade building,” *Energy Build.*, vol. 72, pp. 280–287, 2014.

[16] F. Stazi, F. Tomassoni, A. Vegliò, and C. Di Perna, “Experimental evaluation of ventilated walls with an external clay cladding,” *Renew. Energy*, vol. 36, no. 12, pp. 3373–3385, 2011.

[17] F. Stazi, A. Vegliò, and C. Di Perna, “Experimental assessment of a zinc-titanium ventilated façade in a Mediterranean climate,” *Energy Build.*, vol. 69, pp. 525–534, 2014.

[18] M. N. Sánchez, C. Sanjuan, M. J. Suárez, and M. R. Heras, “Experimental assessment of the performance of

open joint ventilated façades with buoyancy-driven airflow," *Sol. Energy*, vol. 91, pp. 131–144, 2013.

[19] F. Patania, A. Gagliano, F. Nocera, A. Ferlito, and A. Galesi, "Thermofluid-dynamic analysis of ventilated facades," *Energy Build.*, vol. 42, no. 7, pp. 1148–1155, 2010.

[20] F.Stazi, G.Ulpiani, M.Pergolini, D. Magni, C. Di Perna, "Experimental comparison between three types of Opque ventilated facades", Open Construct Build Tech J, vol. 12, pp.296-308, 2018.

[21] J. Yu, J. Yang, C. Xiong, "Study of dynamic thermal performance of hollow block ventilated wall", Renewable Energy, vol. 84, pp. 145-151, 2015.

[22] F.Stazi, G. Ulpiani, M. Pergolini, C. Di Perna, "The role of areal heat capacity and decrement factor in case of hyper insulated buildings: an experimental study", *Energy Build.*, vol. 176, pp.310-324, 2018.

[23] F. Stazi, A. Vegliò, C. Di Perna, "Experimental assessment of a zinc-titanium ventilated façade in a Mediterranean climate", *Energy Build.*, vol. 69, pp.525-534, 2014.

[24] Standard ISO 9869-1:2014 - Thermal insulation - Building elements - In-situ measurement of thermal resistance and thermal transmittance -Part 1: Heat flow meter method.

[25] F. Stazi, "Thermal Inertia in Energy Efficient Building Envelopes", Butterworth-Heinemann 2017.

[26] C. Marinosci, G. Semprini, and G.L. Morini, "Experimental analysis of the summer thermal performances of a naturally ventilated rainscreen façade building", *Energy Build.*, vol. 72, pp. 280-287, 2014.

[27] M. Ciampi, F. Leccese, and G. Tuoni, "Cooling of buildings: energy efficiency improvement through ventilated structures", WIT Transactions on Ecology and the Environment, vol. 62, pp. 199-210, 2003.

[28] A. Gagliano, F. Patania, A. Ferlito, F. Nocera and A. Galesi, "Computational fluid dynamic simulations of natural onvection in ventilated facades", Evaporation, Condensation and Heat transfer, Amimul Ahsan, IntechOpen, 2011.

[29] I. Guillén, V. Gomez-Lozano, J.M. Fran, and P.A. Lopez-Jimenez, "Thermal behavior analysis of different multilayer façade: numerical model versus experimental prototype", *Energy Build.*, vol. 79, pp. 184-190, 2014.

[30] A. Prada, M. Baratieri, and A. Gasparella, "Analysis of the impact of ventilated cavities on the performance of opaque components", Building Simulation Applications, BSA 2013 - 1st IBPSA Italy Conference, pp. 353-361, 2013.

[31] C. Marinosci, P.A. Strachan, G.Semprini, and G.L. Morini, “Empirical validation and modelling of a naturally ventilated rainscreen façade building”, *Energy Build*., vol. 43, pp. 853-863, 2011.

List of captions

Fig.1. West-oriented wall of the mock-up, (a) before and (b) after the application of the ventilated skins.

Fig.2. Cross-section of the three VS prototypes.

Fig.3. Sensor network. Color is used to distinguish probes of different nature. Black boxes indicate the data acquisition components.

Fig.4. Representative Weather conditions during the summer campaign.

Fig.5. Summer thermal profiles of the three prototypes with respect to (a) the external (b) and internal surface temperatures and (c) the heat fluxes.

Fig.6. Comparison of EM and IM ventilated skins in two summer days characterized by (a) high and (b) low wind speeds.

Fig.7. Representative weather conditions during the winter campaign.

Fig.8. Winter thermal profiles of the three prototypes with respect to (a) the external and (b) internal surface temperatures and (c) the heat fluxes.

Fig.9. Comparison of EM and IM ventilated skins in two winter days characterized by (a) low and (b) high wind speeds.

Fig.10. Trends of the average temperatures across EM, IM and L facades for different hours in (a) summer and (b) winter).

List of figures

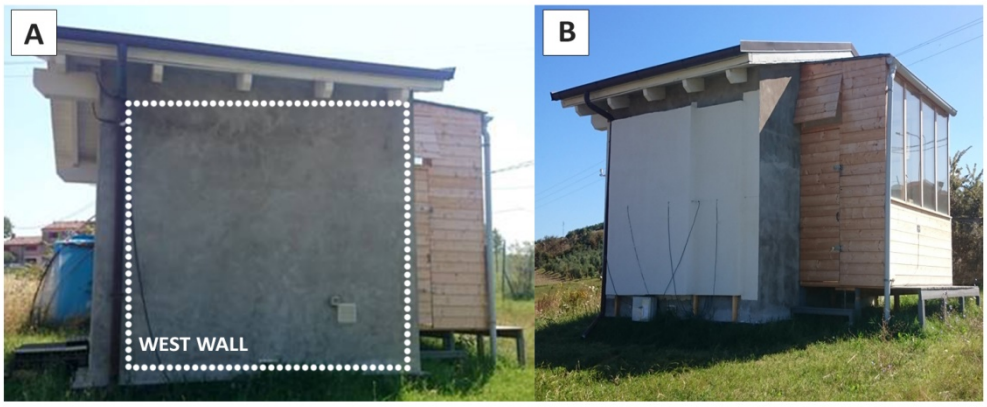

Fig.1. West-oriented wall of the mock-up, (a) before and (b) after the application of the ventilated skins.

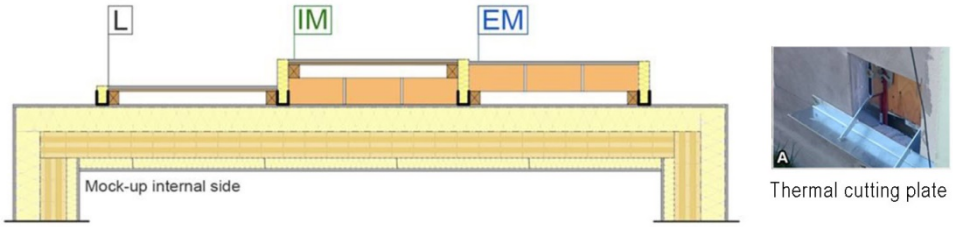

Fig. 2. Cross-section of the three VS prototypes.

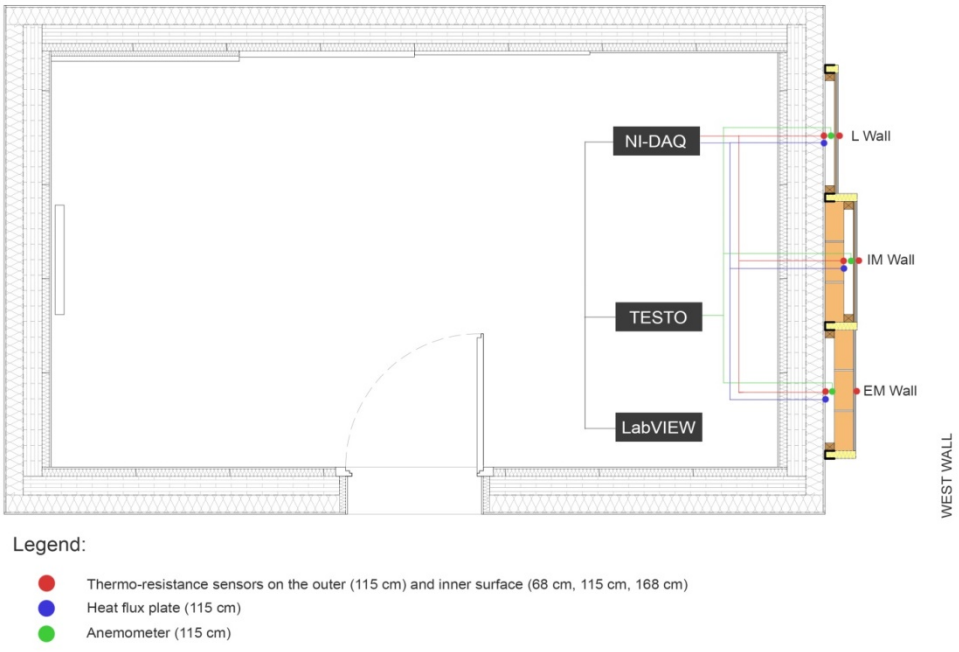

Fig.3. Sensor network. Color is used to distinguish probes of different nature. Black boxes indicate the data acquisition components.

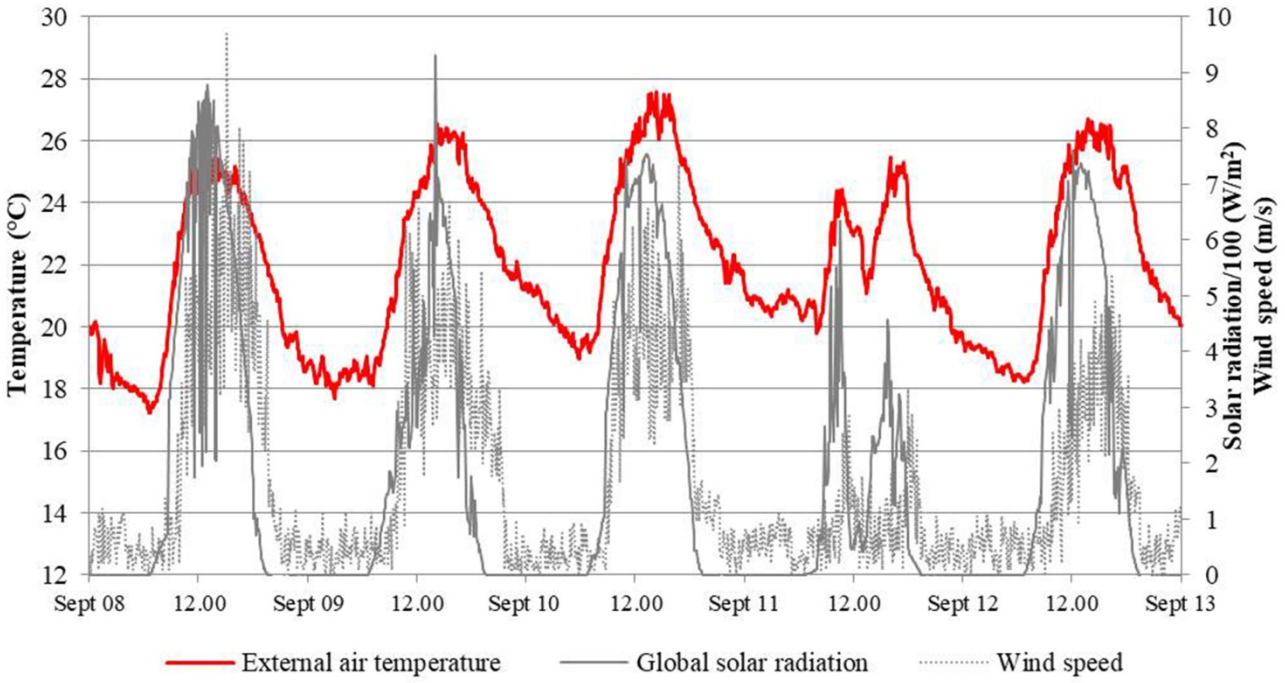

Fig.4. Representative Weather conditions during the summer campaign.

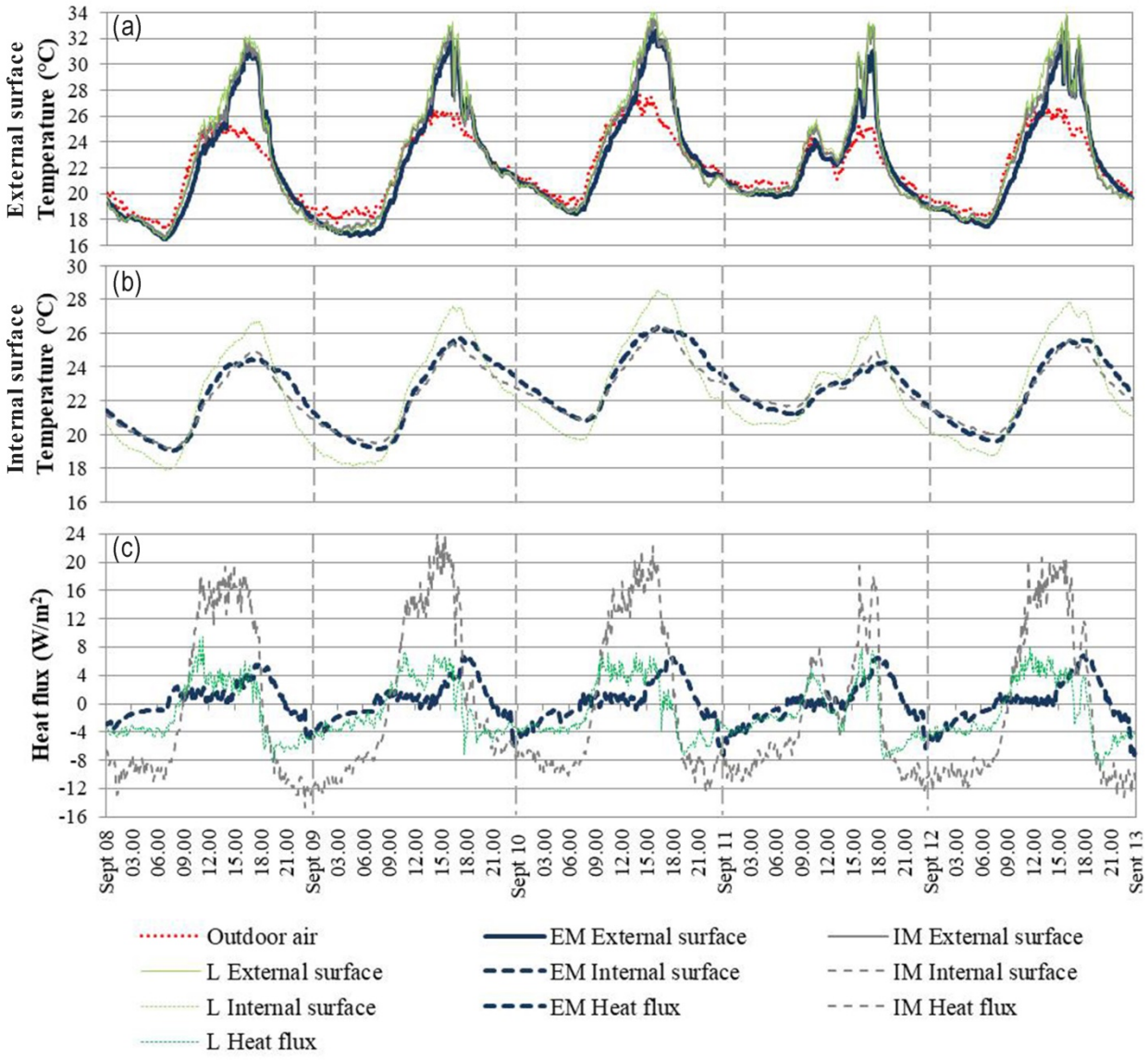

Fig.5. Summer thermal profiles of the three prototypes with respect to (a) the external (b) and internal surface temperatures and (c) the heat fluxes.

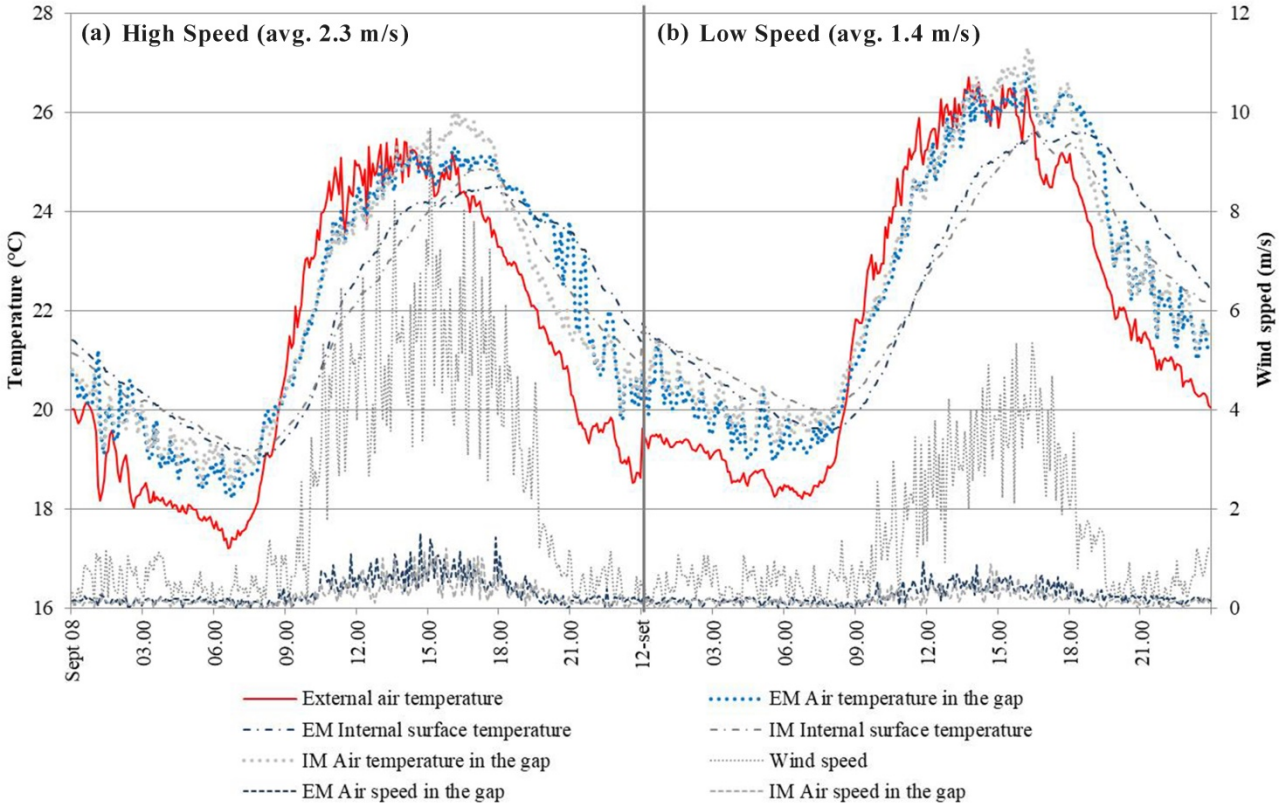

Fig. 6.Comparison of EM and IM ventilated skins in two summer days characterized by (a) high and (b) low wind speeds.

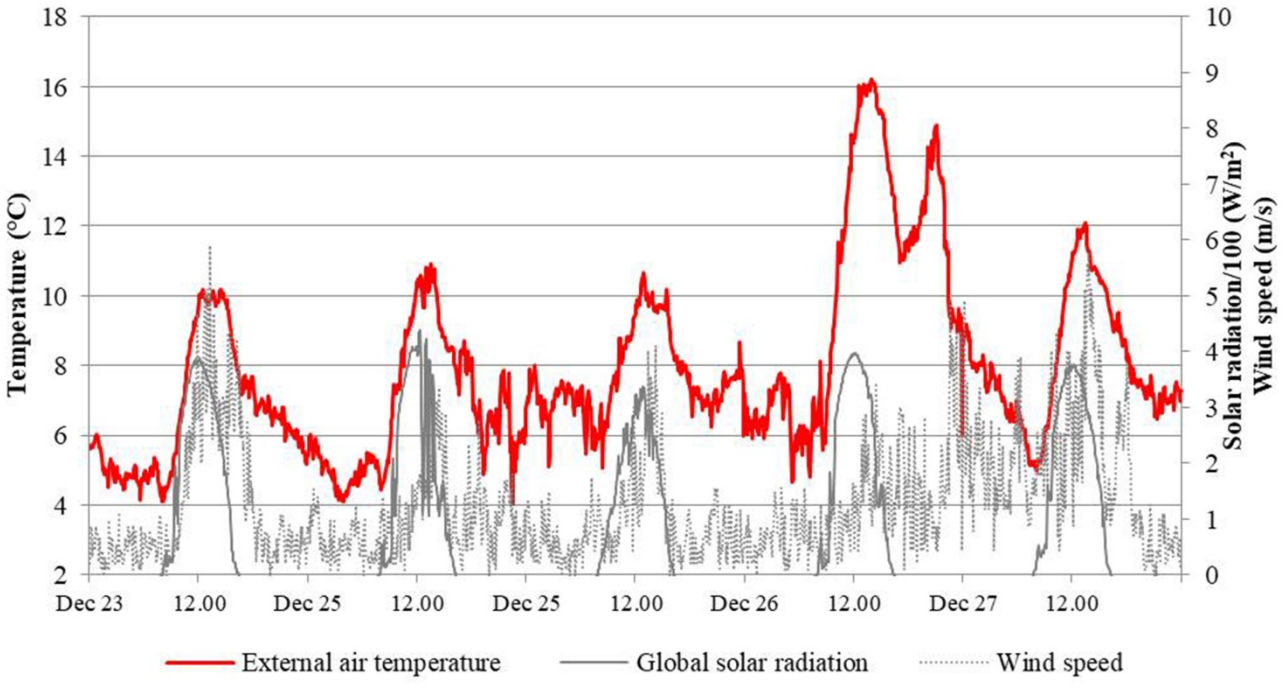

Fig. 7. Representative weather conditions during the winter campaign.

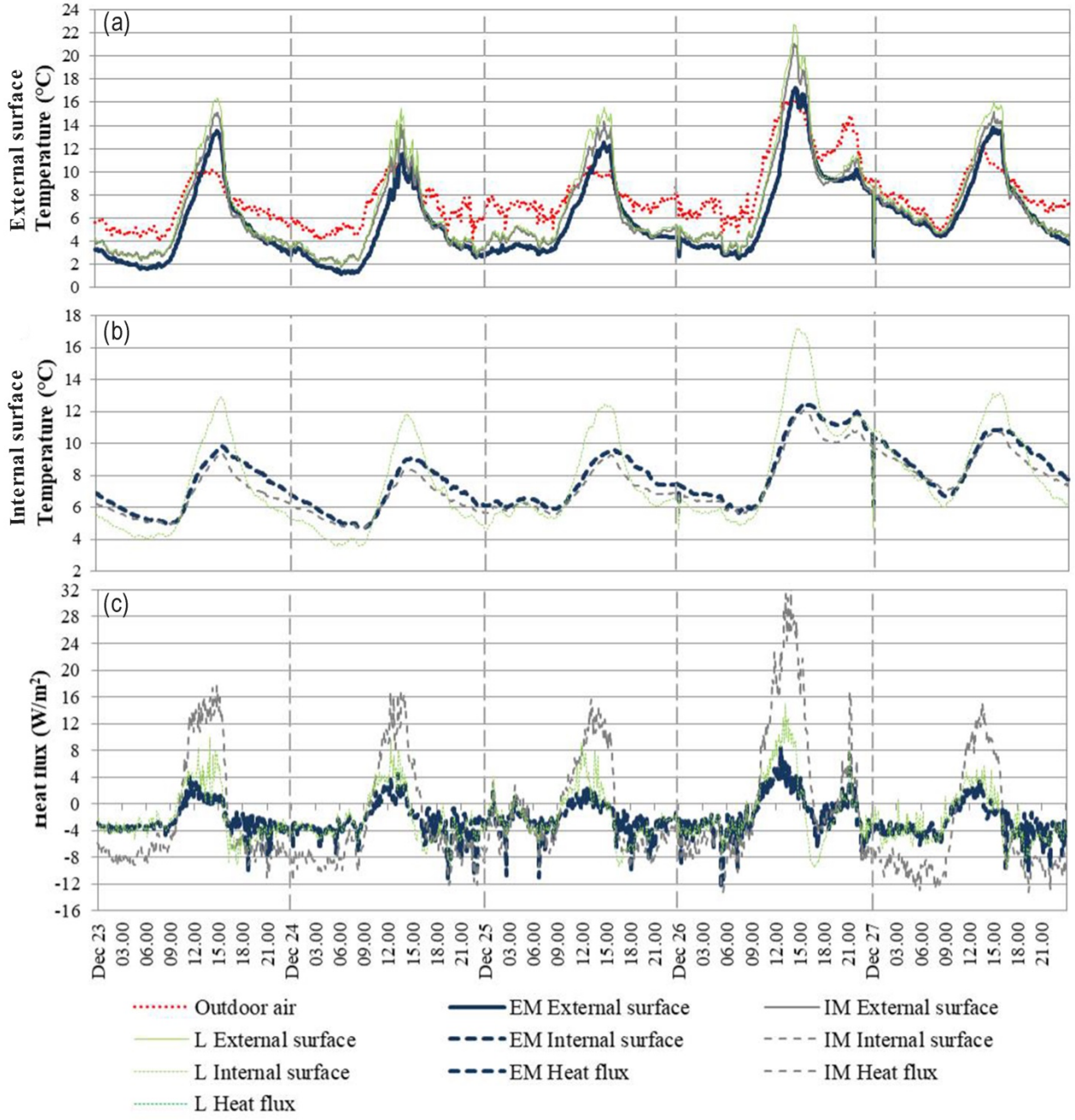

Fig.8. Winter thermal profiles of the three prototypes with respect to (a) the external and (b) internal surface temperatures and (c) the heat fluxes.

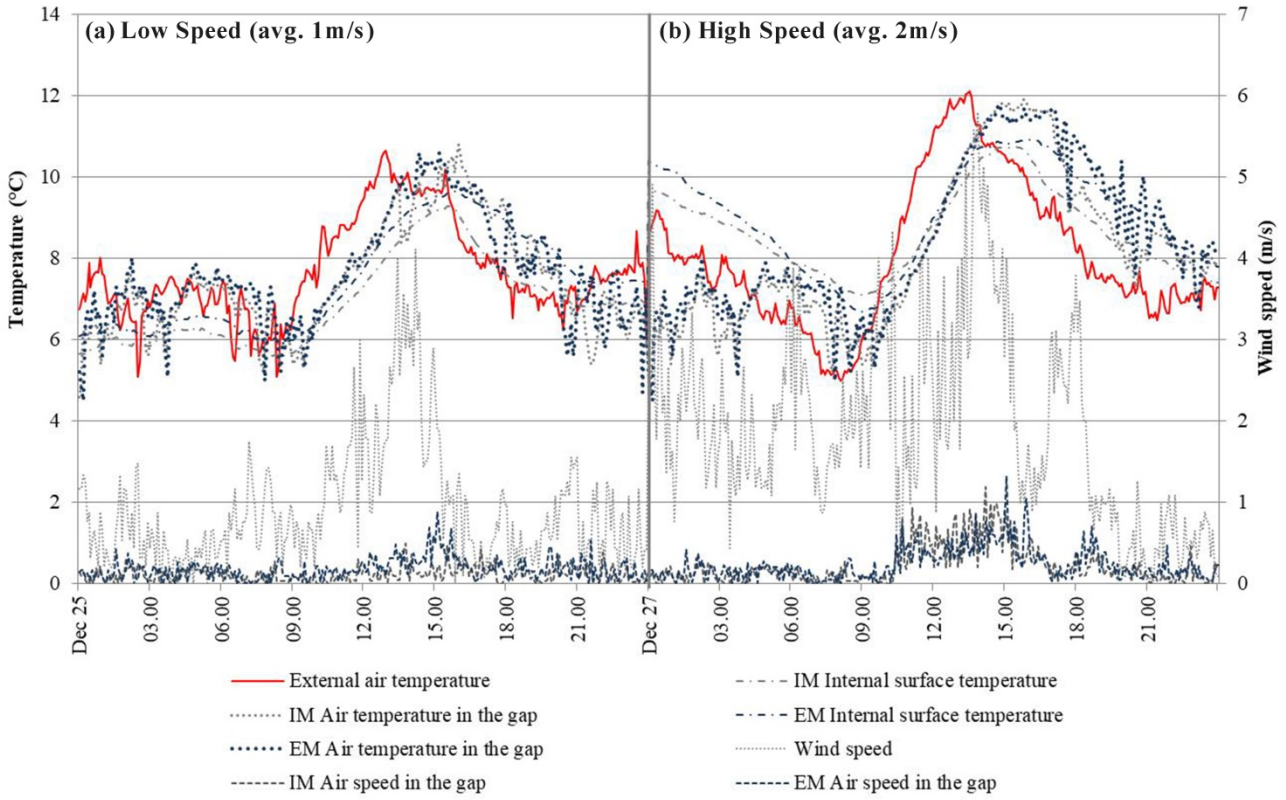

Fig.9. Comparison of EM and IM ventilated skins in two winter days characterized by (a) low and (b) high wind speeds.

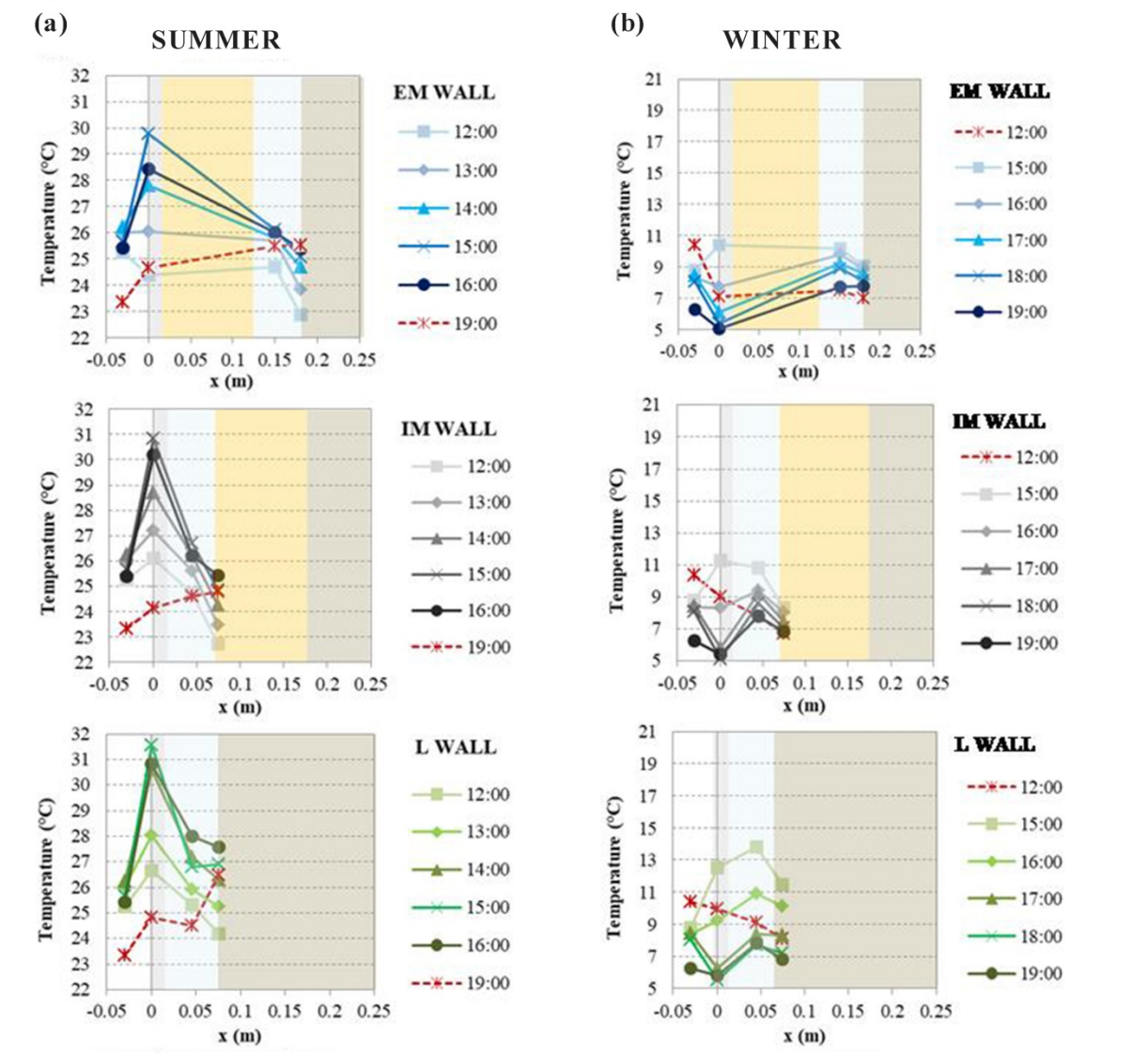

Time (hh:mm)	Solar radiation (W m^{-2})	Wind speed (m s^{-1})	Air gap speed (m/s)		
			EM	IM	L
12:00	298	1.34	0.32	0.18	0.42
13:00	737	3.34	0.57	0.21	0.6
14:00	699	3.67	0.27	0.33	0.35
15:00	613	3.78	0.64	0.16	0.22
16:00	216	3.21	0.47	0.22	0.25
19:00	17	1.48	0.13	0.18	0.19

Time (hh:mm)	Solar radiation (W m^{-2})	Wind speed (m s^{-1})	Air gap speed (m/s)		
			EM	IM	L
12:00	409	1.57	0.29	0.28	0.37
15:00	149	2.33	0.50	0.33	0.72
16:00	16	1.09	0.23	0.23	0.17
17:00	0	0.21	0.19	0.08	0.18
18:00	0	0.44	0.07	0.06	0.2
19:00	0	1.34	0.18	0.05	0.04

Fig.10. Trends of the average temperatures across EM, IM and L facades for different hours in (a) summer and (b) winter).

Tables

Table 1. Composition of the Ventilated Skin prototypes.

	VS with no mass (L)	VS with internal mass (IM)	VS with external mass (EM)
	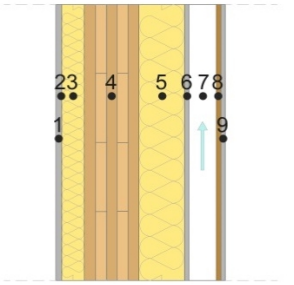	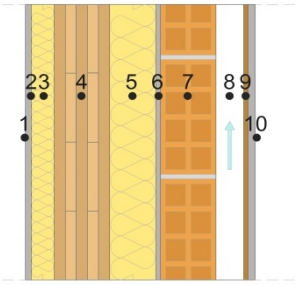	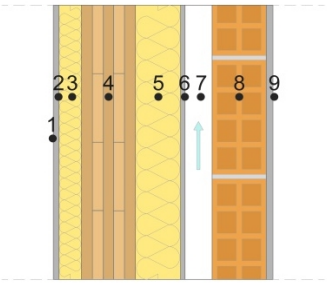
	Layer		
1	Internal Plasterboard	Internal Plasterboard	Internal Plasterboard
2	Vapour Barrier	Vapour Barrier	Vapour Barrier
3	Internal Insulation	Internal Insulation	Internal Insulation
4	Cross laminated timber	Cross laminated timber	Cross laminated timber
5	External Insulation	External Insulation	External Insulation
6	Cement mortar	Cement mortar	Cement mortar
7	Air Cavity	Hollow Brick	Air Cavity
8	OSB Panel	Air Cavity	Hollow Brick
9	External Plaster	OSB Panel	External Plaster
10	-	External Plaster	-

Table 2. Thermo-physical properties of the layers.

Material	**Thickness (m)**	**Thermal conductivity (W/mK)**	**Specific heat capacity (J/kgK)**	**Density (kg/m^3)**
Internal Plasterboard	0.0125	0.2	837	760
Vapour Barrier	-	0.17	1500	425
Internal Insulation	0.05	0.035	1030	70
Cross laminated timber	0.12	1.4	2700	500
External Insulation	0.10	0.036	1030	90
Cement mortar	0.015	0.48	1000	1150
Hollow Brick	0.12	0.292	1000	920
Air Cavity*	0.06	-	-	-
External Plaster	0.012	0.33	1110	1150
OSB Panel	0.009	0.1	1700	600

*Thermal resistance of 0.18 m^{2}K/W

Table 3. VSs' steady state and dynamic thermal parameters.

Thermal Properties	Wall Typology		
	L	**IM**	**EM**
Thermal Transmittance U (W/m^2K) [a, b]	0.22	0.20	0.22
Decrement Factor f^b	0.08	0.04	0.08
Time Lag Δt (h) [b]	8.4	13.9	8.4
Periodic Thermal Trasmittance Y_{12} (W/m^2K) [b]	0.017	0.07	0.017
External Areal Heat Capacity k_2 (kJ/m^2K) [c]	28	40	60

[a] calculated according to EN ISO 6946:2008.
U < 0.26 Wm^2/K according to the Italian regulation on energy efficiency (D.M. 2015).

[b] calculated according to EN ISO 13786:2008, considering a well-ventilated facade by disregarding the outer layer.

[c] calculated according to EN ISO 13786:2008, considering all the envelope layers and still air in the gap to better highlight the role of the external mass.

Table 4. 99th percentile, median and interquartile range (IQR) of the surface temperatures and the heat fluxes during the representative summer period.

	99 Percentile	**Q1**	**Q2**	**Q3**	**IQR**
External surface temperature					
EM	31.74	19.03	21.33	24.79	5.76
IM	32.86	19.11	21.18	25.40	6.29
L	33.29	19.00	21.27	25.92	6.92
Internal surface temperature					
EM	26.19	21.00	22.70	24.18	3.18
IM	26.30	20.99	22.39	23.79	2.81
L	28.21	19.96	22.02	24.81	4.85
Heat fluxes					
EM	6.44	-1.54	0.13	1.58	3.12
IM	21.14	-9.18	-6.08	9.21	18.40
L	6.96	-4.00	-2.62	2.85	6.86

Table 5. 99th percentile, median and interquartile range (IQR) of the surface temperatures and the heat fluxes during the representative winter period.

	99 Percentile	**Q1**	**Q2**	**Q3**	**IQR**
External surface temperature					
EM	16.09	3.29	4.89	8.11	4.82
IM	18.73	4.02	5.16	8.75	4.73
L	19.96	4.14	5.44	9.42	5.28
Internal surface temperature					
EM	12.36	6.29	7.48	9.18	2.89
IM	11.89	5.93	7.02	8.49	2.56
L	16.84	5.46	6.68	10.23	4.77
Heat fluxes					
EM	4.54	-3.62	-2.67	-0.77	2.85
IM	26.34	-7.85	-5.45	2.44	10.29
L	9.71	-4.51	-3.11	0.02	4.53

Highlights

- Investigating the impact of different materials adjacent to the air cavities of ventilated facades;
- Experimental evaluation on three prototypes in summer and winter;
- The thermal mass in the outer side of the gap enhanced the stack effect;
- The thermal mass in the inner side of the gap increased the heat transfer towards the indoor.

Title page

The role of wall layers properties on the thermal performance of ventilated facades: experimental investigation on narrow-cavity design

First author and corresponding author

Francesca Stazi [(a)]

E-mail: f.stazi@univpm.it

Tel: (+39) 3283098217

Second author

Giulia Ulpiani [(b)]

E-mail: g.ulpiani@pm.univpm.it

Third author

Marianna Pergolini [(a)]

E-mail: m.pergolini@hotmail.it

Fourth author

Costanzo Di Perna [(b)]

E-mail: c.diperna@univpm.it

Fifth author

Marco D'Orazio [(c)]

E-mail: m.dorazio@univpm.it

Affiliation

(a) Department of Materials, Environmental Sciences and Urban Planning (SIMAU), Polytechnic University of Marche, Ancona, Italy

(b) Department of Industrial Engineering and Mathematical Sciences (DIISM), Polytechnic University of Marche, Ancona, Italy

(c) Department of Civil, Constructional and Environmental Engineering (DICEA), Polytechnic University of Marche, Ancona, Italy

The role of wall layers properties on the thermal performance of ventilated facades: experimental investigation on narrow-cavity design

F. Stazi[(a)], G. Ulpiani[(b)], M. Pergolini[(a)], C. Di Perna[(b)] , M. D'Orazio [(c)]

(a) Department of Materials, Environmental Sciences and Urban Planning (SIMAU), Polytechnic University of Marche, Ancona, Italy

(b) Department of Industrial Engineering and Mathematical Sciences (DIISM), Polytechnic University of Marche, Ancona, Italy

(c) Department of Civil, Constructional and Environmental Engineering (DICEA), Polytechnic University of Marche, Ancona, Italy

Abstract

In this paper we have investigated how different materials and thermal masses impact on the performance of ventilated facades with narrow cavities, by measuring the variation in terms of heat flows and ventilation efficiency. While geometry has been widely explored, the role of wall composition has received much less attention. To bridge the gap, three real-scale prototypes of ventilated facades were built and tested all over the year on a mock-up in Central Italy: (i) L, with a lightweight external enclosure, as a baseline reference, (ii) IM, with a massive layer enclosed in the gap and (iii) EM, with an external massive cladding. The results demonstrated that the EM solution more effectively mitigated the average surface temperatures (both external and internal), with values of –2°C and -1°C in summer and of -3°C and -0.5°C in winter, when compared to the L solution. Moreover, in the EM case, the ventilated cavity reduced both the incoming and outgoing heat fluxes, since the outer mass operated as a thermal buffer between the outdoor and the ventilation chamber. Conversely, the presence of an internal mass determined an increase of the heat transfer towards the indoor environment. The position of the thermal mass in the outer layer also increased the air velocity in the gap thus enhancing the stack effect.

Keywords: Ventilated facades, Experimental study, Thermal inertia, Energy efficiency, Narrow cavity.

1. Introduction

In the roadmap for a constant pursuit of durability improvement of buildings outer surfaces, Ventilated Skins (VS) were originally conceived as rain screens, finding application in both retrofitting and new buildings interventions. International studies demonstrated that they could also be effective as a passive cooling strategy on annual basis, with respect to the unventilated option [1-9].

The ventilated skin is an external coating system, secured to the building envelope by means of mechanical anchoring points. It consists of four functional layers (from the inner side to the outer side): (i) internal layer; (ii) continuous insulation layer; (iii) ventilation chamber with lower and upper openings connected to the outdoor air; (iv) external cladding [10, 11]. Many parameters influence the air gap behavior and, ultimately, the impacts on the building energy budget. They can be divided in two main categories:

- outdoor boundary conditions, such as geographical localization [12], solar radiation [13] and wind speed [14];
- design choices, namely width and height of the ventilation gap [15], external cladding material [16,17] and joints configuration that can be either open [18] or closed [19]. These research studies focused on the evaluation of one single facade typology, but no study concerned the simultaneous comparison between walls with different external VS solutions.

The ventilated skin is an efficient system for both summer and winter. In the summertime, the thermal gradient between upper and lower openings activates the air flow (driven by buoyancy and wind forces) allowing the heated air in the ventilation chamber to be expelled through the outlet opening, hence reducing the heat gains toward the indoors [6, 10, 12, 14, 20]. In the wintertime, the ventilation gap behaves as a thermal buffer that accumulates heat and dampens the temperature difference between inside and outside, thus curbing transmission losses. Moreover, it positively affects the thermal resistance of the wall. This aspect was rarely investigated in existing studies [21, 22].

The key purpose of the present experimental research was to determine the impact of different materials adjacent to the air cavity on the heat fluxes and ventilation efficacy. Three prototypes were experimentally tested, simultaneously: one lightweight with plastered OSB panel (hereafter termed “L”), one with internal mass and the same external lightweight OSB panel (“IM”) and one with external massive cladding through the use of hollow bricks (“EM”). Extensive measurements were collected and analyzed to compare the thermo-physical performance and natural ventilation potential, with respect to the buoyancy and wind forces. For each prototype, the following parameters were measured: the surface temperature on the outer side of the façade and on the inner side of the gap, the heat fluxes, the air speed and the temperature in the gap.

2. Experimental method

2.1 Ventilated Skin prototypes

The experiment was carried out in Agugliano, Central Italy, featuring Csa climatic conditions according to the K□ppen-Geiger classification: the hottest month is August (average temperature around 32°C) and the coldest one is January (average temperature around 8°C).

The skins were mounted on the western façade of an experimental mock-up (Fig. 1a), exposed to direct sunlight over the hottest afternoon hours and thus being more susceptible to overheating [23].

The mock-up is representative of a full-scale, single rectangular room (net area of 12.2 m^2). The load bearing structure is made of cross laminated timber panels. The building is highly insulated, with insulation layers placed both on the external and the internal sides. Also, it is unoccupied and windowless to avoid unequal contributions of the solar radiation and uncontrollable internal heat gains. The wall composition is detailed in Table 1 (see layers 1-6). The thermal transmittance, measured *in-situ* according to the Standard ISO 9869 [24], is 0.13 W/m^2K.

The west-facing wall of the mock-up covers 9 m^2 (3.22 m length x 2.80 m height). Three rectangular-shaped ventilated skins were tailor-made to fit in the available surface (Fig.1b), with each modulus of 1 m length x 2.30 m height, raised 30 cm off the ground.

As specified in Table 1, the L configuration featured an aerated gap (layer 7) enclosed by a white plastered, oriented strand board (OSB) (layers 8-9) and it was used as reference for comparisons. The IM configuration had a massive layer (7) in between the insulation material and the air gap, while the EM configuration exhibited the massive layer (8) on the outer side of the air gap, finished with white plaster (9).

For all the facades, a narrow cavity was selected (0.06 m width) to emphasize the contribution of different materials enclosing the gap. Moreover, this value is intermediate among the most common [11] and it is the most suitable solution for the selected metallic substructure.

The white plaster was intentionally adopted for the three outer skins as to prevent any bias due to different optical properties. The emissivity was 0.9 and the solar reflectance was 0.60. The thermo-physical properties of the abovementioned materials, given by the manufactures, are presented in Table 2 while Fig. 2 shows the cross section of the three prototypes.

The facades were assembled using vertical wooden batten support frames, and bottom steel supporting brackets screwed to the cross laminated timber structure, coupled with thermal cutting plates to eliminate thermal bridges (Fig. 2, insert A). XPS insulation layers were sealed on either side of each wall to enclose the air chambers. Honey-combed nets were placed to protect the cavities.

Standards EN ISO 6946:2008 and EN ISO 13786:2008 were adopted for the characterization of the thermal parameters of the three ventilated modules, considering a well ventilated air chamber (Table 3). L and EM enclosures show equal thermal features, given that the calculation disregards the thermal resistance of the air layer and all the other layers between the air gap and the external environment. Table 3 also reports the values of the external areal heat capacity $\boldsymbol{k}_2$ (obtained according to the same standards) but including all the layers in the calculation. In this case, the three prototypes showed increasing levels of inertia, from the lowest value of L (28 kJ/m^{2}K) to the highest one of EM (60 kJ/m^{2}K).

External and internal surface temperatures and heat fluxes data were analyzed by means of the following statistic distribution measures in order to avoid outliers:

- 99th percentile to indicate the maximum value;
- The median (Q2) to indicate the middle value;
- The interquartile range (IQR) as the difference between the upper (Q3) and lower (Q1) quartiles to describe the values spread.

2.2 Sensors network

The monitoring activity was carried out throughout the year in order to examine the thermal behavior of the ventilated skins during different seasons. A set of devices was installed to record:

1. Outdoor temperature, relative humidity, global solar radiation, speed and direction of the wind. Data were collected using a weather station, 3 m away from the ventilated facades;
2. Surface temperatures of the outermost and innermost layers at the bottom (60 cm), middle (115 cm) and top (168 cm) of each façade. Thermo-resistance sensors (accuracy ± 0,05 °C) were adopted;
3. Incoming and outgoing heat fluxes at mid-height (115 cm) in the innermost side of the air chamber, measured by heat flux plates (accuracy ± 3%);
4. Air velocity and air temperature inside the ventilation chamber at mid-height (115 cm). Data were collected using TESTO hot-sphere anemometers (accuracy ±0.03 m/s).

The output analog signals from the probes were digitized by means of NI-DAQ acquisition modules. LabVIEW was used to manage the dataflow and its elaboration. The acquisition rate was 5 minutes. The sensor network was arranged as displayed in Fig. 3.

3. Summer results

This paragraph shows the results from the experimental campaign in summertime. Fig. 4 provides an overview of the weather conditions of 5 consecutive days, representative of the typical Mediterranean summer climate.

3.1 Surface temperature and fluxes

The external surface temperatures profiles are plotted in Fig. 5a. We used data collected in September since, as demonstrated elsewhere [22, 25], the thermal inertia benefits are better appreciated in periods characterized by cooler nights, since the mass is able to cool itself properly. Indeed, we noticed that the differences between the three experimented walls were more significant in September. As expected, the values recorded at 115 cm were always significantly higher than the ambient air. Moreover, when the sun hit the western façade in the afternoon (14:00 – 18:00), the values notably increased, with an average offset of 7°C. EM showed daily peaks almost 2°C lower than the other two configurations over the hottest hours (see September 12th). All the surface temperatures plummeted overnight. The EM solution touched the absolute minima since the outer mass released the stored heat outwards, without showing any conservative behavior.

Fig. 5b reports the surface temperatures measured on the innermost side of the cavity at mid-height (115 cm). L experienced the greatest thermal range, reaching daytime maxima (exceeding the ones of the outdoor air when the sun hit the façade) and the minima by night (very close to the outdoor air). By contrast, EM and IM showed milder fluctuations. EM registered the lower values throughout the day since it dissipated, in a more effective way, the retained heat. These observations got confirmed by the statistical analysis in Table 4, that shows how EM guaranteed temperature reductions of about 4.7% on the external surface and of 7.2% on the internal one, compared to L.

The thermal flux trends for the three walls (recorded at mid-height, on the inner side of the air gap), are shown in Fig. 5c. The heat fluxes are positive with an incoming direction towards the test room. Around peak hours (11:00 – 16:00), the IM prototype flux reached the highest values, compared to those recorded by the other two. This might be explained by considering that, for this wall only, the heat flux plate measured the storing action, since it was placed directly on the hollow bricks. In contrast, the EM heat flux was negligible in the morning and increased only later in the afternoon (with an inward direction). The mass positioned on the external side of the air gap operated as a thermal buffer between the outdoors and the ventilation chamber, strongly mitigating the driving force for heat transmission.

Therefore, it required more time before an appreciable thermal gradient could be spotted on the edge of the air gap, triggering the heat flow. In the evening, the heat flow reversed (negative sign). In particular, heat fluxes of IM and L suddenly dropped with very similar slopes while EM underwent a milder decline because of the external mass inertial storing action. The reduction of the heat coming from the outside between EM and IM approached 70 % (Table 4).

3.2 Wind action and stack effect in summer

EM and IM were compared in terms of airflow rate in two summer days (Fig.6), namely September 8th and 12th, characterized by similar daily average solar radiation (around 400 W/m^2) but different wind speeds (averages of 2.3 m/s and 1.4 m/s, respectively), coming from the same prevalent direction for the selected site (North).

The air speed profiles in the gaps followed the wind trends: the stack effect was accentuated in the windiest day for both configurations with a 30% velocity bump with respect to the unventilated day (Fig.6). Consequently, the temperatures of the internal surface and the air within both the cavities diminished.

However, unequal wind speed values did not alter significantly the distance among the temperature curves characterizing the two walls. The EM internal surface temperature curve was always lower than the other, except in the morning hours (10:00-15:00 time slot), and it reached the highest maximum peak between 15:00 and 18:00. Furthermore, the air temperatures in the gaps almost coincided, until 15:00. IM showed greater fluctuations, reaching the highest maximum value and descending with a more tilted trend.

4. Winter results

The present section illustrates the results obtained from the winter monitoring campaign. A representative set of the outdoor boundary conditions in the coldest months is showed in Fig. 7.

4.1 Surface temperature and fluxes

The winter temperature trends of the external surfaces, recorded at mid height (115 cm), are presented in Fig. 8a. All the temperatures were higher than the outdoor air in the middle of the day. L reached again the highest values, with peaks approximately 1°C above IM. The EM external surface temperature remained the coolest throughout the day lowering the daily peaks down to 5°C on the warmest day (December 26th) with respect to the others. During the nighttime, the outer surface temperatures of the three walls dropped significantly. As in summertime, EM stayed around 2°C cooler than the other configurations since the outer mass could completely cool itself. In the morning hours, this led to a significant difference (around 3°C) between the rising outdoor temperature and EM surface temperature.

Fig.8b reports the surface temperatures on the innermost side of the gap. The curves confirmed the summer trends, with less pronounced fluctuations for the massive walls and more emphasized for the lightweight solution. As demonstrated by the statistical analysis in Table 5, the surface temperature reduction between L and EM is more noticeable than in summer, touching –20% and -27% for the external and internal surface temperatures, respectively.

The daily heat flux trends were very similar to those recorded in summertime (Fig. 8c) with EM always recording the minima.

4.2 Wind action and stack effect in winter

The airflow rates of EM and IM were compared on two different days (Fig.9), namely December 25th and 27th, characterized by similar daily average solar radiation (200 W/m^2) but different wind speeds (average values of 2 m/s and 1 m/s, respectively), again in the north direction.

The same observations made in 3.2 could be drawn also for the winter season (Fig. 9). Even in winter, the air speed trends in the gaps followed the wind fluctuations and, as expected, the stack effect was more pronounced in the windiest day for both the massive configurations. The mean air speeds within the cavity were 0.17-0.22 m/s for EM and 0.11-0.20 m/s for IM. As the wind force was halved, also the average air velocities in the gap of both walls experienced a reduction of nearly 50%. The air speed in the ventilation gap was negligible at night while it reached the highest values over peak hours. Nonetheless, the relative behavior between the two walls was maintained. The EM internal surface temperature stayed always higher than the other one, notably during the afternoon hours. Conversely, the air temperatures within the gaps had almost the same trends.

5. Discussion

The present work deals with the effect of adopting different materials in the boundaries of the ventilated gap, in the case of narrow cavities, in summer and winter. It was experimentally demonstrated that the use of massive layers is beneficial in terms of temperature reduction: both prototypes with high mass within the cavity (EM and IM) exhibited reduced internal surface temperatures in the inner side of the gap and lower air gap temperatures, with respect to the solution with lightweight materials (L). Moreover, the mass should be preferably positioned on the outer side of the cavity (EM) guaranteeing lower incoming/outgoing fluxes and higher stack effect with respect the internal mass solution (IM).

This result is novel in literature, yet well in accordance with previous researches. Indeed, while the most common studies vary the type of the external cladding (e.g. aluminum, terracotta, etc.) and the thermal resistance of the

internal layers, more rare are the researches that address the effect of the change of the mass position with respect to the cavity (internal or external side).

The change of the external cladding (e.g. stone cladding rather than aluminum) has demonstrated to affect both the chimney effect efficacy and the long-wave thermal radiation within the air cavity as a result of the change of the radiative properties of the exterior finishing [26]. Other research that envisaged the comparison between alternative materials was carried out by Ciampi et al. [27]. In particular, changing only the external claddings from massive terra cotta to lightweight copper, they demonstrated that the former is the most convenient from the energy point of view.
Some other authors, by comparing facades with very different layers stressed that the performance of the façade is influenced by the repartition of thermal resistance between the layers on the inner and outer sides of the cavity [28]. They introduced a dimensionless parameter *z*, representing the fraction of thermal resistance facing the external environment and demonstrated its correlation with the incoming heat fluxes through the ventilated façades and ventilation efficacy. The higher the parameter *z*, the more efficient the ventilation. For the prototypes of the present study, this parameter is about 9% for EM wall and around 3% for IM and L walls, thus confirming their findings.

The change of the thermal properties of the layer on the internal side of the cavity was instead addressed by Guillen et al. [29]. In particular, they analyzed the effect of the increase of the insulation level of the internal layers. This affected both the thermal periodic transmittance and the time lag but no mention was done on the effect of this change on the cavity performance. Another investigation in this topic was carried out by Prada et al. [30]. They compared two cases, one with insulation behind the cavity and one considering a not insulated mass. Moreover, they changed the emissivity of the cavity inner surface to deepen its effect on the air motion and heat transfer. They highlighted that the insulated wall reached higher air velocities for the entire wall height. This result is also confirmed by our data (see table in Fig.10) regarding winter and summer air velocities in the cavities for all the three prototypes. The L solution, even if characterized by high summer temperatures and winter crossing fluxes, exhibits a good stack effect all year round.

The abovementioned studies are commonly based on analytical comparisons and mainly aimed at highlighting the effect of different cavity geometries. Moreover, at the author's knowledge, no studies focused on the comparison of alternative configurations using the same materials and under the same optical properties for the external finishing but modifying the mass position. The present research aims at filling the highlighted gap through experimental data. This study is intentionally focused on narrow cavities since several authors demonstrated that the materials adjacent to a restricted gap have higher influence on its energy balance and ventilation efficacy [11].

Even in mild climates as Mediterranean's, the construction sector is moving towards higher and higher insulation levels, thus decoupling the behavior of the internal environment from the external one and ascribing this

relationship to the windows rather than to the opaque wall. As a consequence, we have adopted a hyper-insulated envelope and have focused exclusively on the outer side of the opaque wall to gain insight into the behavior of the cavity only with respect to its adjacent layers, facing outwards.

The results are synthetized and comparatively evaluated in Fig.10, that reports the hourly temperatures for a single summer (September 12th) and winter (December 24th) day, by superimposing the data to the walls sections. The temperature values recorded outdoors, in the outer surface, in the air cavity and in the innermost side of the gap are plotted during the central day hours for both seasons. Hourly values of air cavity velocity, global solar radiation and wind speed are also reported in the tables within the figure.

In the warmest season (Fig. 10a), the peak on the outer skin was recorded at 15:00 for all the facades, with L reaching the absolute maximum. Low air temperatures within the cavity are desirable to maximize the heat expulsion through the envelope [31]. This was the case of the massive configurations (EM and IM) that recorded almost the same temperature range (25°C-26.5°C), differently by L wall that reached values up to 28°C. Hence, the adoption of a thermal mass in contact with the air gap, irrespectively of the relative position, could be beneficial in terms of heat transfer reduction.

Even in the coldest season, EM recorded the lowest air cavity temperatures (Fig.10b). L reached higher surface temperatures only during the central hours of the day, peaking around midday, while in the evening it behaved similarly to the other two claddings. It could be concluded that the EM configuration recorded a more homogeneous behavior, both in summer and winter, with air temperatures in the gap and air speeds almost uniform throughout the day, and with the lowest internal surface temperatures in summer.

These results are obtained for the climate of Agugliano, characterized by a hot dry summer Mediterranean climate. In summer the average temperatures are about 23°C while in winter they drop down to 9°C. However, more detailed studies on the replicability of the results in other climatic contexts should be addressed.

6. Conclusion

The present experimental research was carried out with the purpose of establishing the impact of different boundary conditions on the year-round behavior of narrow cavities in ventilated facades. Three real-scale prototypes were designed and simultaneously monitored on a mock-up in Central Italy: one with a lightweight external cladding as reference (L), one with a massive layer in the innermost side of the air gap and a lightweight finishing (IM) and one with an outer massive enclosure (EM). Extensive measurements were conducted in summer and winter in order to identify the trends of the surface temperatures, the airflow rate in the gaps, and the heat fluxes.

It was experimentally demonstrated that the EM facade exhibited the coolest external and internal surface temperatures and the lowest incoming heat fluxes. The outer mass operated as a thermal buffer between the outdoors and the ventilation chamber hence reducing the incoming and outgoing heat fluxes through the envelope both in summer and winter. Moreover, the insertion of a thermal mass in the outer layer increased the air velocity in the gap hence emphasizing the stack effect. Also the internal mass IM was beneficial in terms of surface temperature, but it facilitated the heat transfer towards the indoor environment, thus incrementing summer gains.

Therefore, it was concluded that the adoption of a massive material in the outer side of a narrow gap (EM prototype) represented the optimal solution on annual basis, considering both the thermo-physical performance and the natural ventilation potential. Further investigation will address the potential for energy savings, also considering other materials and under condition of controlled air speeds.

Acknowledgements

The research was supported by HALFEN Company and by StilCasa Costruzioni. A particular thank to Eng. Andi Celaj, for the construction of the ventilated prototypes. The authors also want to express their gratitude to CENTROLEGNO and in particular to its CEO Roberto del Bianco, for the provision of the cross laminated timber test room.

REFERENCES

[1] C. Rosenzweig, W. D. Solecki, L. Parshall, M. Chopping, G. Pope, and R. Goldberg, “Characterizing the urban heat island in current and future climates in New Jersey,” *Environ. Hazards*, vol. 6, no. 1, pp. 51–62, 2005.

[2] M. Santamouris, “Regulating the damaged thermostat of the cities—Status, impacts and mitigation challenges,” *Energy Build.*, vol. 91, pp. 43–56, Mar. 2015.

[3] E. Di Giuseppe, M. Pergolini, and F. Stazi, “Numerical assessment of the impact of roof reflectivity and building envelope thermal transmittance on the UHI effect,” *Energy Procedia*, vol. 134, no. 2016, pp. 404–413, 2017.

[4] Y. Wang, U. Berardi, and H. Akbari, “Comparing the effects of urban heat island mitigation strategies for Toronto, Canada,” *Energy Build.*, vol. 114, pp. 2–19, 2016.

[5] M. Santamouris *et al.*, “On the energy impact of urban heat island in Sydney: Climate and energy potential of mitigation technologies,” *Energy Build.*, vol. 166, pp. 154–164, 2018.

[6] M. Santamouris, “Using cool pavements as a mitigation strategy to fight urban heat island - A review of the actual developments,” *Renew. Sustain. Energy Rev.*, vol. 26, pp. 224–240, 2013.

[7] P. Seferis, P. Strachan, A. Dimoudi, and A. Androutsopoulos, “Investigation of the performance of a ventilated wall,” *Energy Build.*, vol. 43, no. 9, pp. 2167–2178, 2011.

[8] M. Ciampi, F. Leccese, and G. Tuoni, “Cooling of buildings: Energy efficiency improvement through ventilated structures,” vol. 7, no. January 2003, pp. 199–210, 2003.

[9] M. Shahrestani *et al.*, “Experimental and numerical studies to assess the energy performance of naturally ventilated PV façade systems,” *Sol. Energy*, vol. 147, pp. 37–51, 2017.

[10] D. Bikas, K. Tsikaloudaki, K. J. Kontoleon, C. Giarma, S. Tsoka, and D. Tsirigoti, “ScienceDirect Ventilated Facades: Requirements and Specifications Across Europe,” *Procedia Environ. Sci.*, vol. 38, pp. 148–154, 2017.

[11] M. Ibañez-Puy, M. Vidaurre-Arbizu, J. A. Sacristán-Fernández, and C. Martín-Gómez, “Opaque Ventilated Façades: Thermal and energy performance review,” *Renew. Sustain. Energy Rev.*, vol. 79, no. May, pp. 180–191, 2017.

[12] F. Peci López and M. Ruiz de Adana Santiago, “Sensitivity study of an opaque ventilated façade in the winter season in different climate zones in Spain,” *Renew. Energy*, vol. 75, pp. 524–533, 2015.

[13] E. Iribar-Solaberrieta, C. Escudero-Revilla, M. Odriozola-Maritorena, A. Campos-Celador, and C. García-Gáfaro, “Energy performance of the opaque ventilated facade,” *Energy Procedia*, vol. 78, pp. 55–60, 2015.

[14] A. Gagliano, F. Nocera, and S. Aneli, “Thermodynamic analysis of ventilated façades under different wind conditions in summer period,” *Energy Build.*, vol. 122, pp. 131–139, 2016.

[15] C. Marinosci, G. Semprini, and G. L. Morini, “Experimental analysis of the summer thermal performances of a naturally ventilated rainscreen facade building,” *Energy Build.*, vol. 72, pp. 280–287, 2014.

[16] F. Stazi, F. Tomassoni, A. Vegliò, and C. Di Perna, “Experimental evaluation of ventilated walls with an external clay cladding,” *Renew. Energy*, vol. 36, no. 12, pp. 3373–3385, 2011.

[17] F. Stazi, A. Vegliò, and C. Di Perna, “Experimental assessment of a zinc-titanium ventilated façade in a Mediterranean climate,” *Energy Build.*, vol. 69, pp. 525–534, 2014.

[18] M. N. Sánchez, C. Sanjuan, M. J. Suárez, and M. R. Heras, “Experimental assessment of the performance of

open joint ventilated façades with buoyancy-driven airflow," *Sol. Energy*, vol. 91, pp. 131–144, 2013.

[19] F. Patania, A. Gagliano, F. Nocera, A. Ferlito, and A. Galesi, "Thermofluid-dynamic analysis of ventilated facades," *Energy Build.*, vol. 42, no. 7, pp. 1148–1155, 2010.

[20] F.Stazi, G.Ulpiani, M.Pergolini, D. Magni, C. Di Perna, "Experimental comparison between three types of Opque ventilated facades", Open Construct Build Tech J, vol. 12, pp.296-308, 2018.

[21] J. Yu, J. Yang, C. Xiong, "Study of dynamic thermal performance of hollow block ventilated wall", Renewable Energy, vol. 84, pp. 145-151, 2015.

[22] F.Stazi, G. Ulpiani, M. Pergolini, C. Di Perna, "The role of areal heat capacity and decrement factor in case of hyper insulated buildings: an experimental study", *Energy Build.*, vol. 176, pp.310-324, 2018.

[23] F. Stazi, A. Vegliò, C. Di Perna, "Experimental assessment of a zinc-titanium ventilated façade in a Mediterranean climate", *Energy Build.*, vol. 69, pp.525-534, 2014.

[24] Standard ISO 9869-1:2014 - Thermal insulation - Building elements - In-situ measurement of thermal resistance and thermal transmittance -Part 1: Heat flow meter method.

[25] F. Stazi, "Thermal Inertia in Energy Efficient Building Envelopes", Butterworth-Heinemann 2017.

[26] C. Marinosci, G. Semprini, and G.L. Morini, "Experimental analysis of the summer thermal performances of a naturally ventilated rainscreen façade building", *Energy Build*., vol. 72, pp. 280-287, 2014.

[27] M. Ciampi, F. Leccese, and G. Tuoni, "Cooling of buildings: energy efficiency improvement through ventilated structures", WIT Transactions on Ecology and the Environment, vol. 62, pp. 199-210, 2003.

[28] A. Gagliano, F. Patania, A. Ferlito, F. Nocera and A. Galesi, "Computational fluid dynamic simulations of natural onvection in ventilated facades", Evaporation, Condensation and Heat transfer, Amimul Ahsan, IntechOpen, 2011.

[29] I. Guillén, V. Gomez-Lozano, J.M. Fran, and P.A. Lopez-Jimenez, "Thermal behavior analysis of different multilayer façade: numerical model versus experimental prototype", *Energy Build*., vol. 79, pp. 184-190, 2014.

[30] A. Prada, M. Baratieri, and A. Gasparella, "Analysis of the impact of ventilated cavities on the performance of opaque components", Building Simulation Applications, BSA 2013 - 1st IBPSA Italy Conference, pp. 353-361, 2013.

[31] C. Marinosci, P.A. Strachan, G.Semprini, and G.L. Morini, “Empirical validation and modelling of a naturally ventilated rainscreen façade building”, *Energy Build*., vol. 43, pp. 853-863, 2011.

List of captions

Fig.1. West-oriented wall of the mock-up, (a) before and (b) after the application of the ventilated skins.

Fig.2. Cross-section of the three VS prototypes.

Fig.3. Sensor network. Color is used to distinguish probes of different nature. Black boxes indicate the data acquisition components.

Fig.4. Representative Weather conditions during the summer campaign.

Fig.5. Summer thermal profiles of the three prototypes with respect to (a) the external (b) and internal surface temperatures and (c) the heat fluxes.

Fig.6. Comparison of EM and IM ventilated skins in two summer days characterized by (a) high and (b) low wind speeds.

Fig.7. Representative weather conditions during the winter campaign.

Fig.8. Winter thermal profiles of the three prototypes with respect to (a) the external and (b) internal surface temperatures and (c) the heat fluxes.

Fig.9. Comparison of EM and IM ventilated skins in two winter days characterized by (a) low and (b) high wind speeds.

Fig.10. Trends of the average temperatures across EM, IM and L facades for different hours in (a) summer and (b) winter).

List of figures

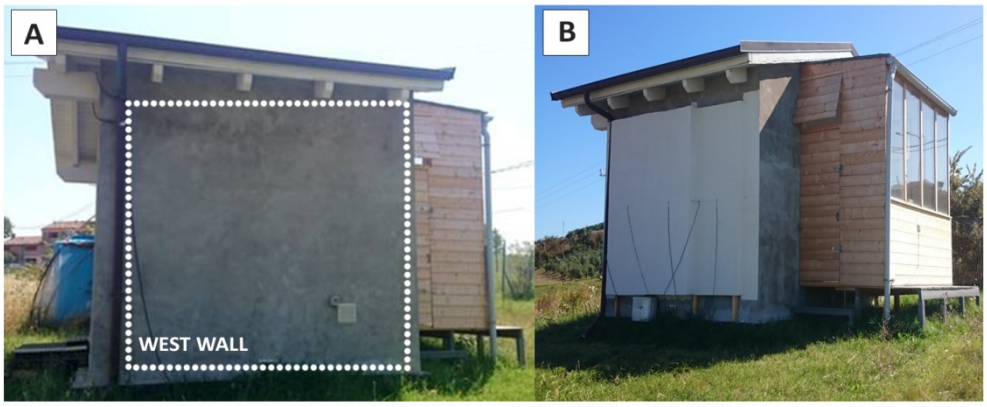

Fig.1. West-oriented wall of the mock-up, (a) before and (b) after the application of the ventilated skins.

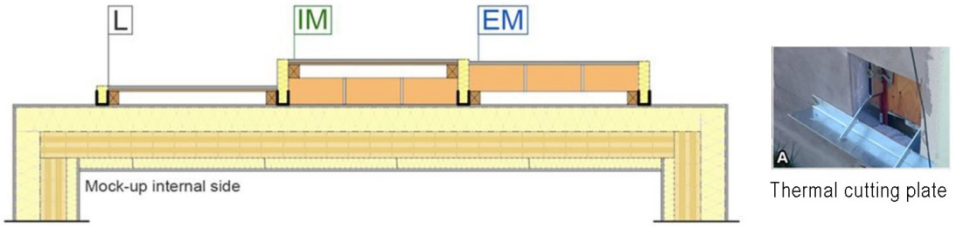

Fig. 2. Cross-section of the three VS prototypes.

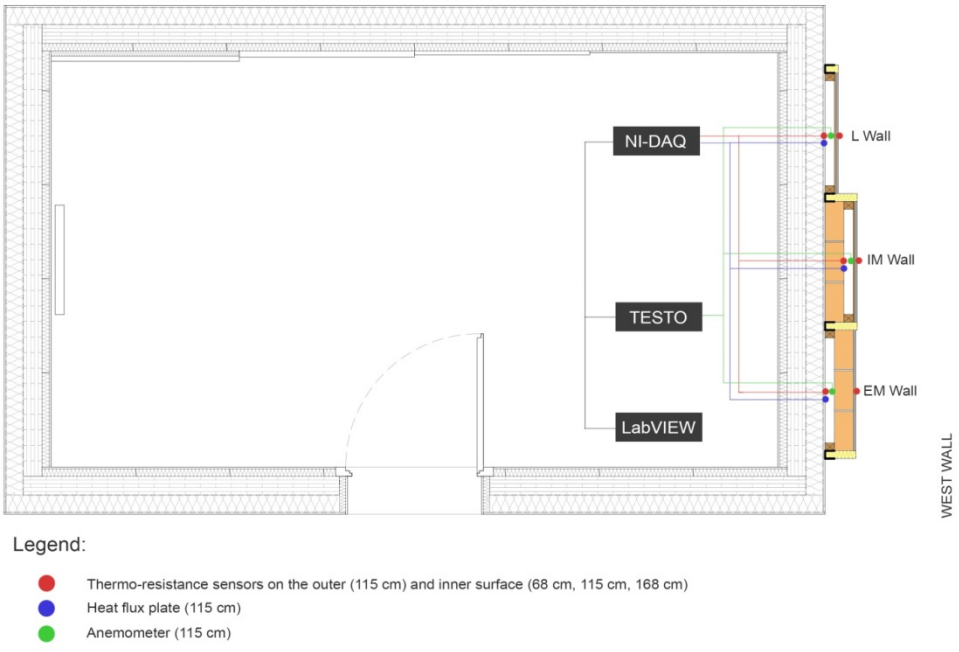

Fig.3. Sensor network. Color is used to distinguish probes of different nature. Black boxes indicate the data acquisition components.

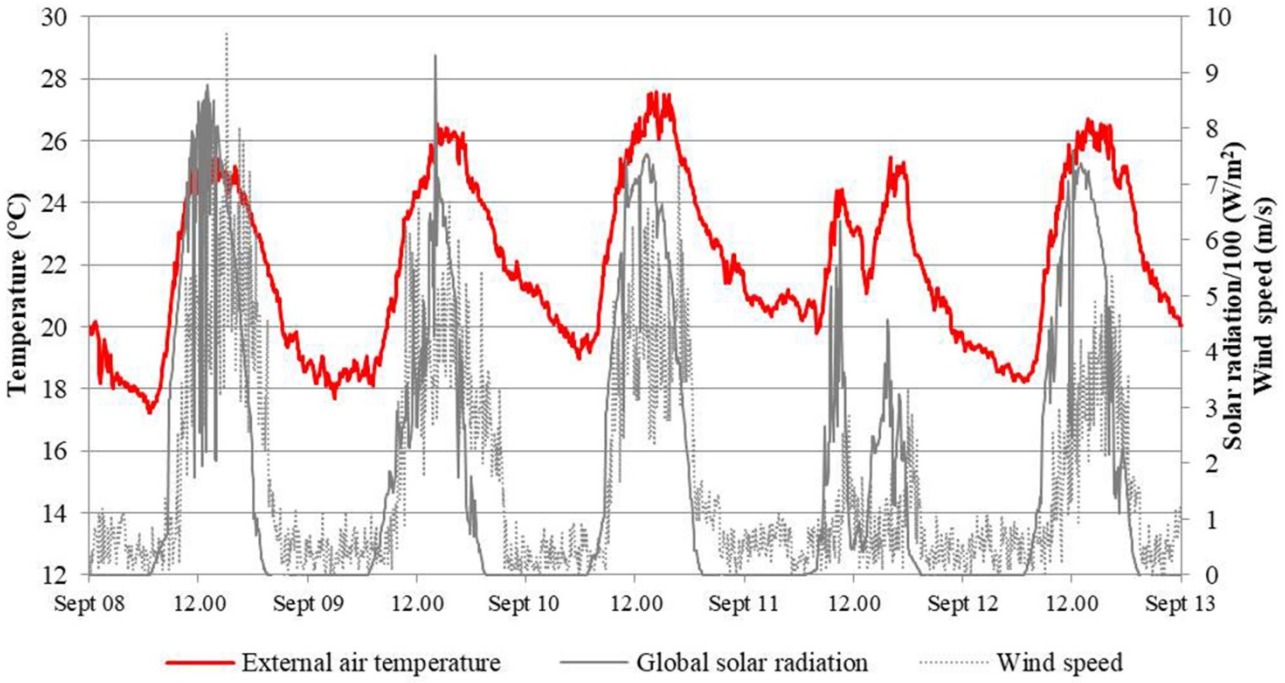

Fig.4. Representative Weather conditions during the summer campaign.

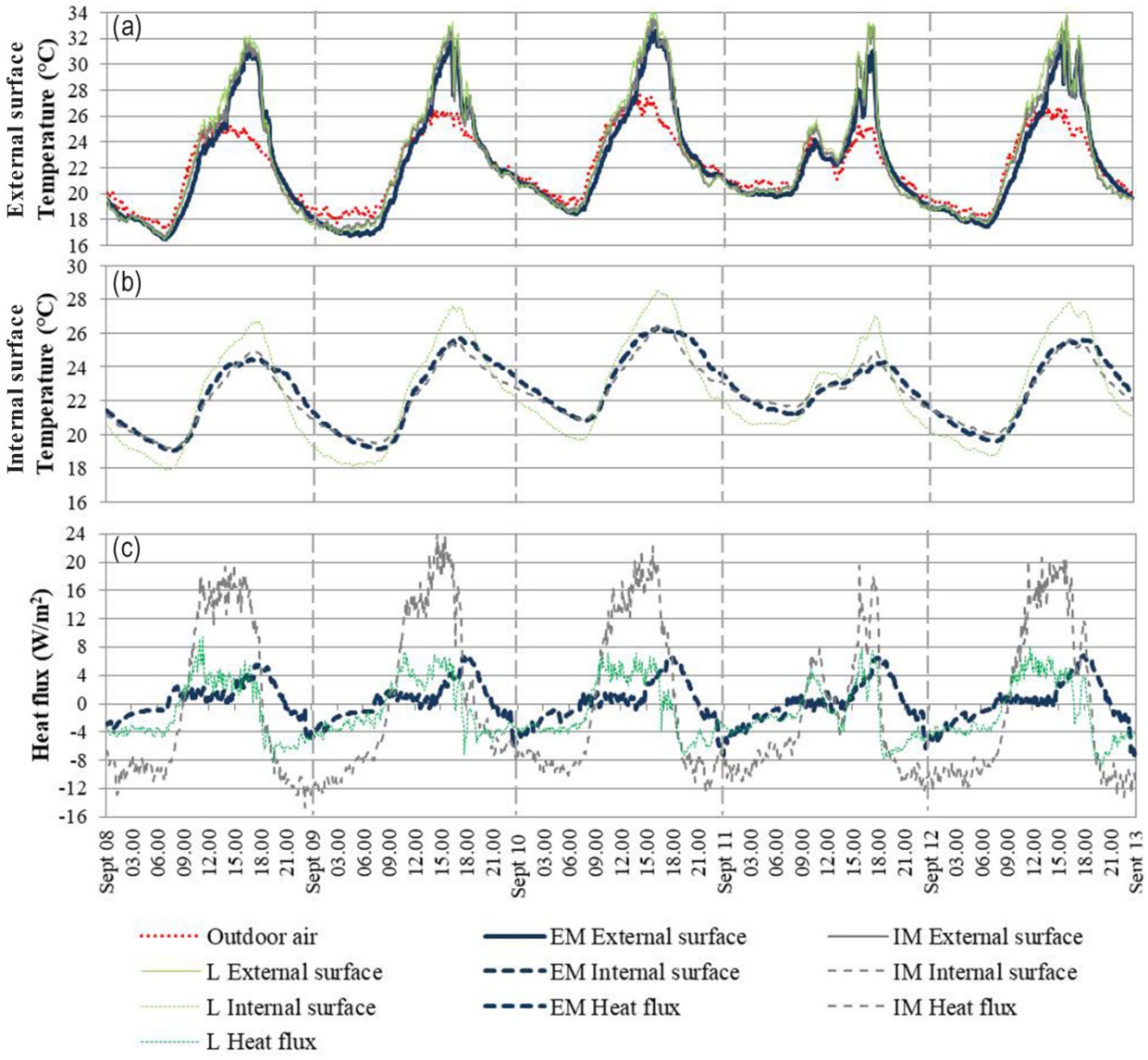

Fig.5. Summer thermal profiles of the three prototypes with respect to (a) the external (b) and internal surface temperatures and (c) the heat fluxes.

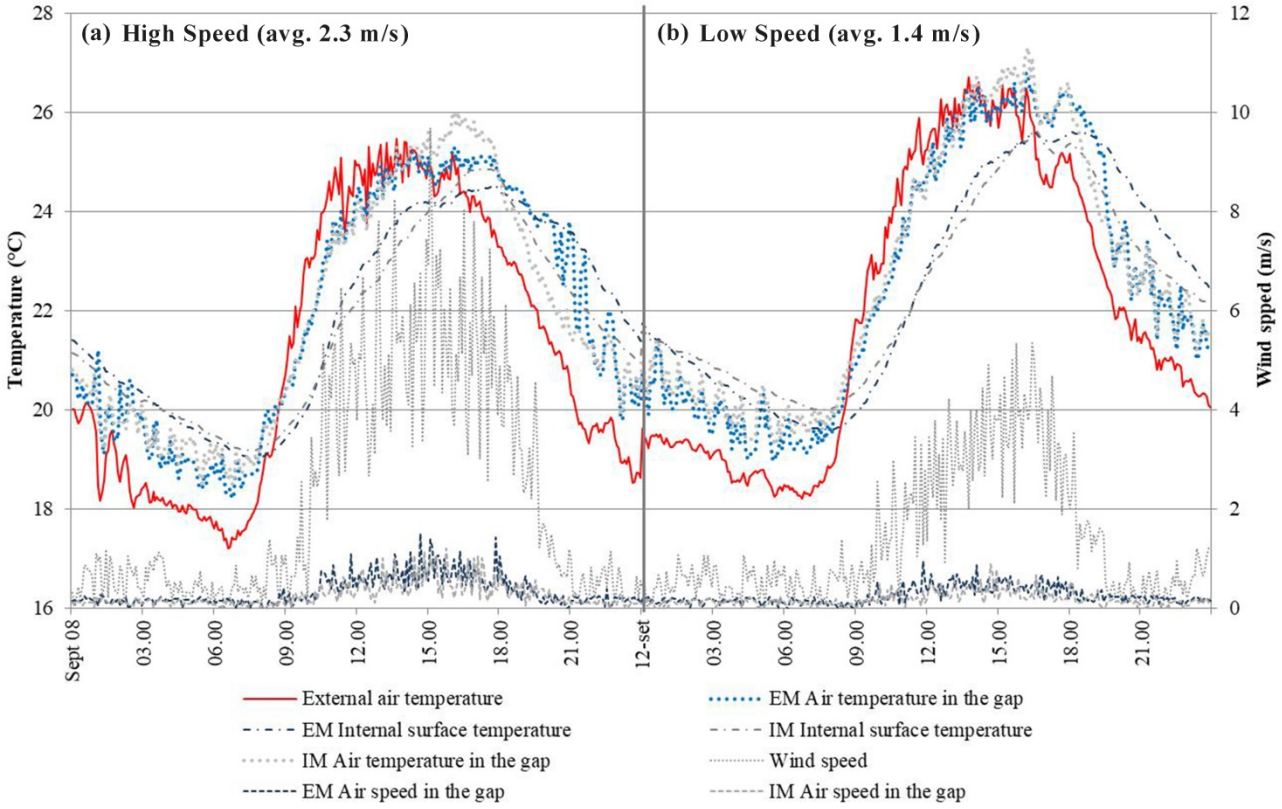

Fig. 6.Comparison of EM and IM ventilated skins in two summer days characterized by (a) high and (b) low wind speeds.

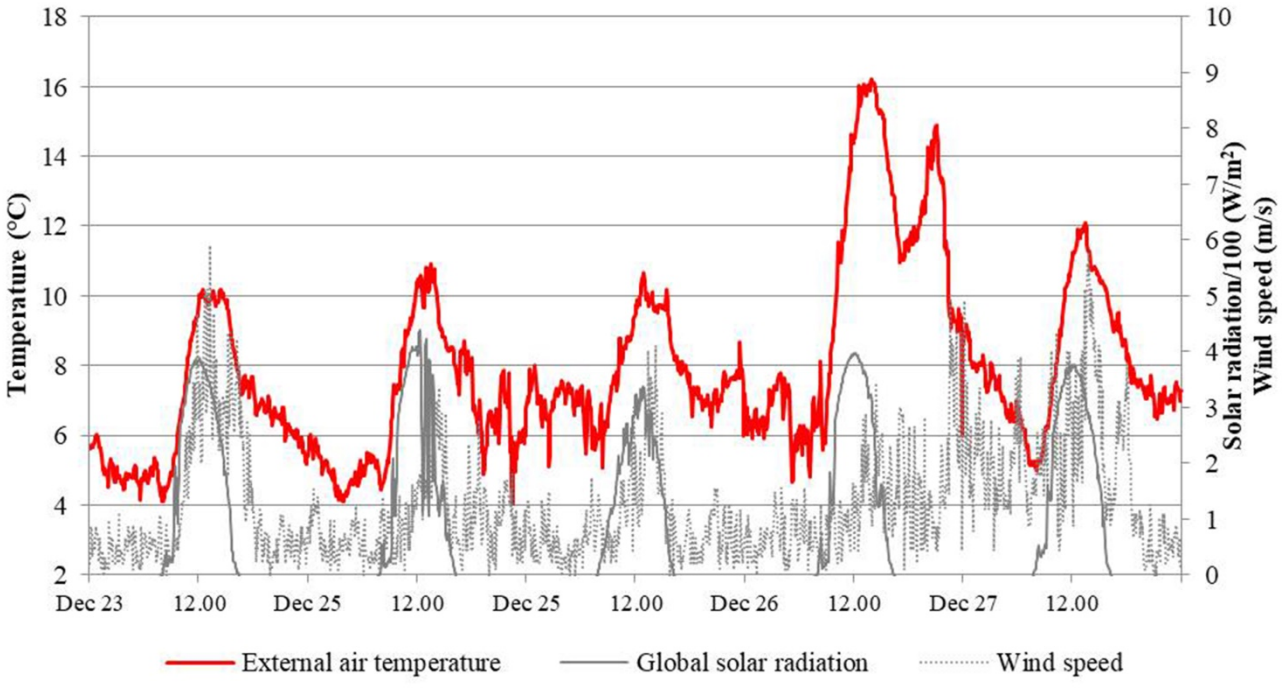

Fig. 7. Representative weather conditions during the winter campaign.

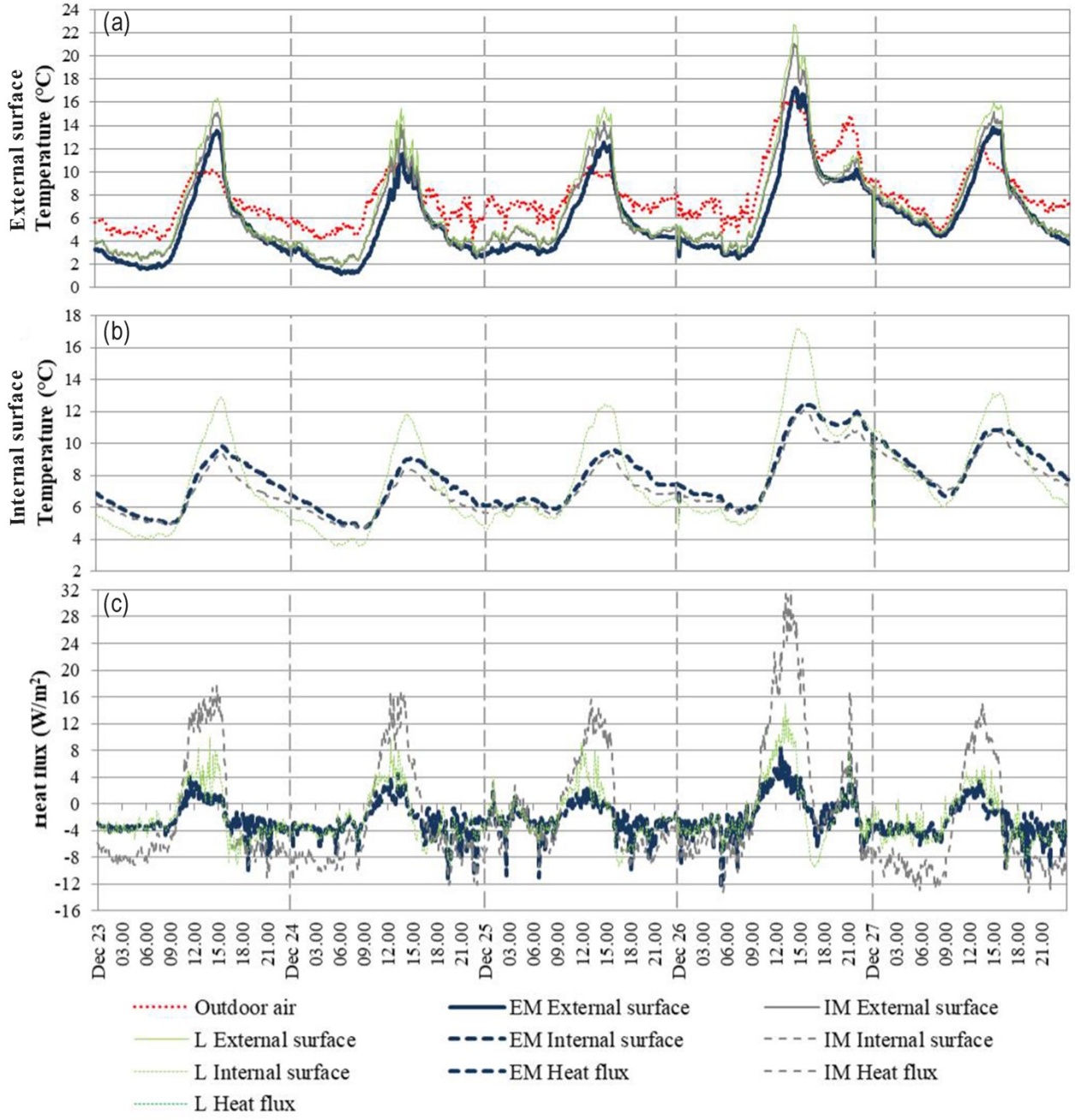

Fig.8. Winter thermal profiles of the three prototypes with respect to (a) the external and (b) internal surface temperatures and (c) the heat fluxes.

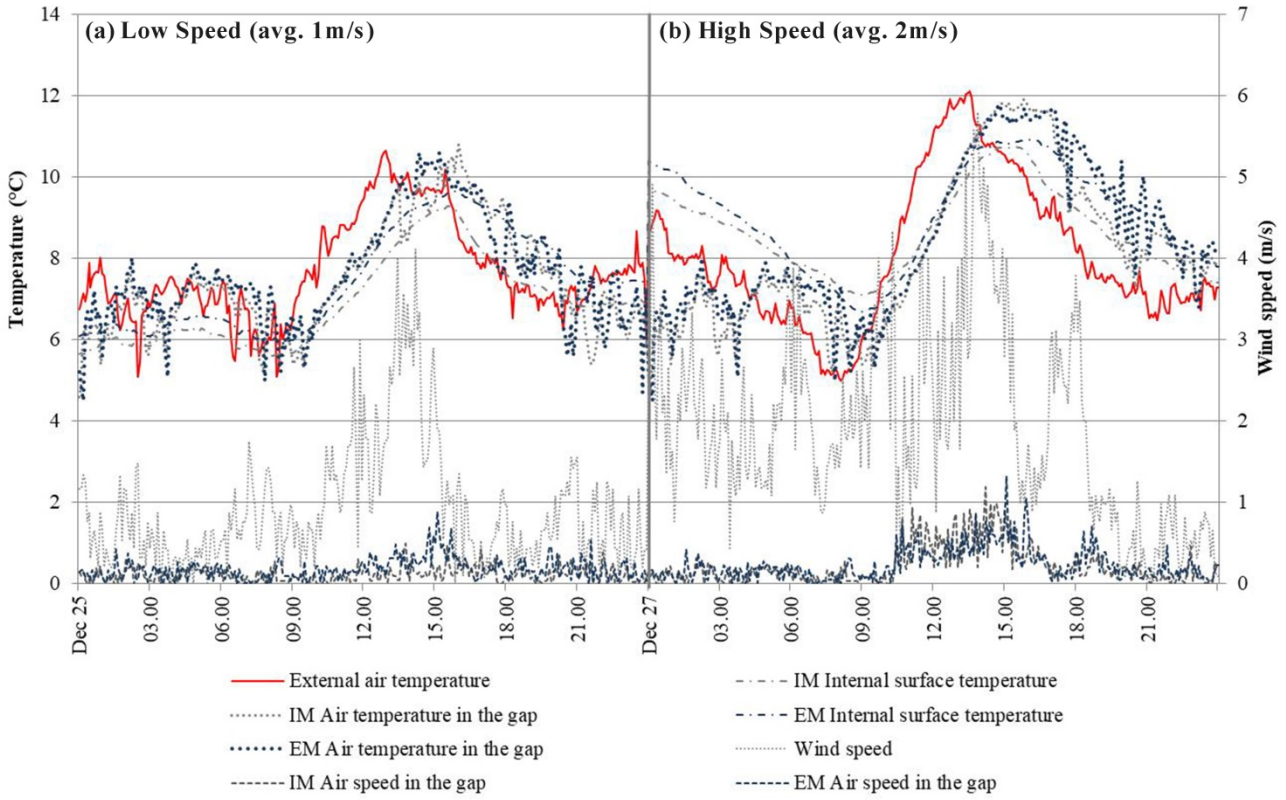

Fig.9. Comparison of EM and IM ventilated skins in two winter days characterized by (a) low and (b) high wind speeds.

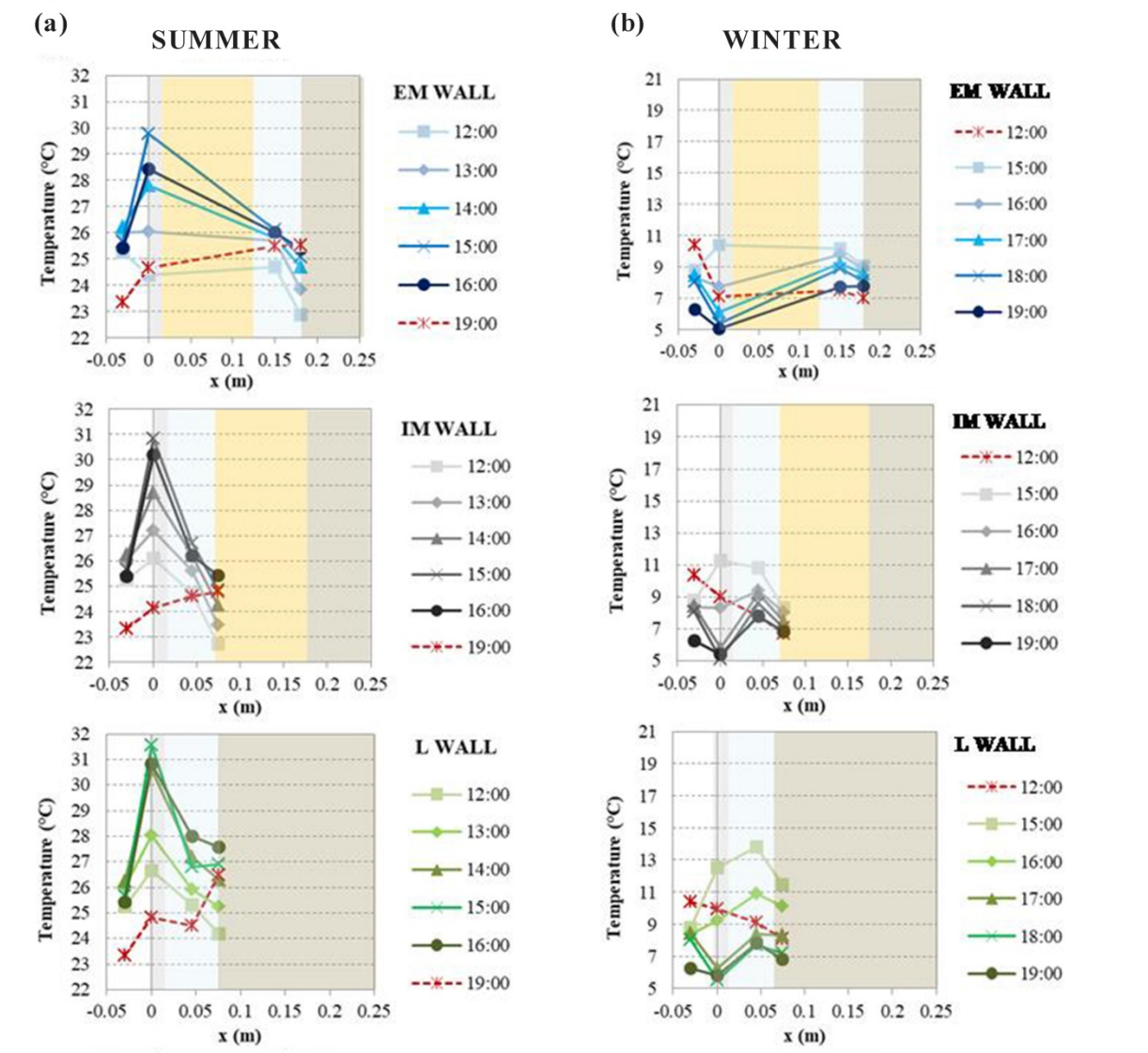

Time (hh:mm)	Solar radiation (W m^{-2})	Wind speed (m s^{-1})	Air gap speed (m/s)		
			EM	IM	L
12:00	298	1.34	0.32	0.18	0.42
13:00	737	3.34	0.57	0.21	0.6
14:00	699	3.67	0.27	0.33	0.35
15:00	613	3.78	0.64	0.16	0.22
16:00	216	3.21	0.47	0.22	0.25
19:00	17	1.48	0.13	0.18	0.19

Time (hh:mm)	Solar radiation (W m^{-2})	Wind speed (m s^{-1})	Air gap speed (m/s)		
			EM	IM	L
12:00	409	1.57	0.29	0.28	0.37
15:00	149	2.33	0.50	0.33	0.72
16:00	16	1.09	0.23	0.23	0.17
17:00	0	0.21	0.19	0.08	0.18
18:00	0	0.44	0.07	0.06	0.2
19:00	0	1.34	0.18	0.05	0.04

Fig.10. Trends of the average temperatures across EM, IM and L facades for different hours in (a) summer and (b) winter).

Tables

Table 1. Composition of the Ventilated Skin prototypes.

	VS with no mass (L)	VS with internal mass (IM)	VS with external mass (EM)
	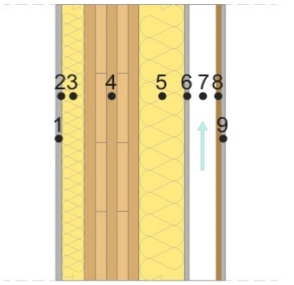	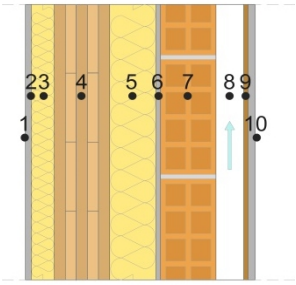	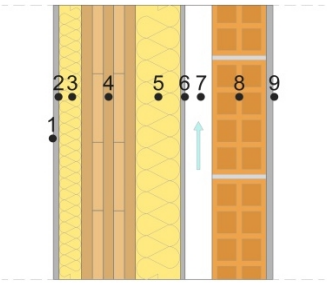
	Layer		
1	Internal Plasterboard	Internal Plasterboard	Internal Plasterboard
2	Vapour Barrier	Vapour Barrier	Vapour Barrier
3	Internal Insulation	Internal Insulation	Internal Insulation
4	Cross laminated timber	Cross laminated timber	Cross laminated timber
5	External Insulation	External Insulation	External Insulation
6	Cement mortar	Cement mortar	Cement mortar
7	Air Cavity	Hollow Brick	Air Cavity
8	OSB Panel	Air Cavity	Hollow Brick
9	External Plaster	OSB Panel	External Plaster
10	-	External Plaster	-

Table 2. Thermo-physical properties of the layers.

Material	**Thickness (m)**	**Thermal conductivity (W/mK)**	**Specific heat capacity (J/kgK)**	**Density (kg/m^3)**
Internal Plasterboard	0.0125	0.2	837	760
Vapour Barrier	-	0.17	1500	425
Internal Insulation	0.05	0.035	1030	70
Cross laminated timber	0.12	1.4	2700	500
External Insulation	0.10	0.036	1030	90
Cement mortar	0.015	0.48	1000	1150
Hollow Brick	0.12	0.292	1000	920
Air Cavity*	0.06	-	-	-
External Plaster	0.012	0.33	1110	1150
OSB Panel	0.009	0.1	1700	600

*Thermal resistance of 0.18 m^{2}K/W

Table 3. VSs' steady state and dynamic thermal parameters.

Thermal Properties	Wall Typology		
	L	**IM**	**EM**
Thermal Transmittance U (W/m^2K) [a, b]	0.22	0.20	0.22
Decrement Factor f^b	0.08	0.04	0.08
Time Lag Δt (h) [b]	8.4	13.9	8.4
Periodic Thermal Trasmittance Y_{12} (W/m^2K) [b]	0.017	0.07	0.017
External Areal Heat Capacity k_2 (kJ/m^2K) [c]	28	40	60

[a] calculated according to EN ISO 6946:2008.
U < 0.26 Wm^2/K according to the Italian regulation on energy efficiency (D.M. 2015).

[b] calculated according to EN ISO 13786:2008, considering a well-ventilated facade by disregarding the outer layer.

[c] calculated according to EN ISO 13786:2008, considering all the envelope layers and still air in the gap to better highlight the role of the external mass.

Table 4. 99th percentile, median and interquartile range (IQR) of the surface temperatures and the heat fluxes during the representative summer period.

	99 Percentile	**Q1**	**Q2**	**Q3**	**IQR**
External surface temperature					
EM	31.74	19.03	21.33	24.79	5.76
IM	32.86	19.11	21.18	25.40	6.29
L	33.29	19.00	21.27	25.92	6.92
Internal surface temperature					
EM	26.19	21.00	22.70	24.18	3.18
IM	26.30	20.99	22.39	23.79	2.81
L	28.21	19.96	22.02	24.81	4.85
Heat fluxes					
EM	6.44	-1.54	0.13	1.58	3.12
IM	21.14	-9.18	-6.08	9.21	18.40
L	6.96	-4.00	-2.62	2.85	6.86

Table 5. 99th percentile, median and interquartile range (IQR) of the surface temperatures and the heat fluxes during the representative winter period.

	99 Percentile	**Q1**	**Q2**	**Q3**	**IQR**
External surface temperature					
EM	16.09	3.29	4.89	8.11	4.82
IM	18.73	4.02	5.16	8.75	4.73
L	19.96	4.14	5.44	9.42	5.28
Internal surface temperature					
EM	12.36	6.29	7.48	9.18	2.89
IM	11.89	5.93	7.02	8.49	2.56
L	16.84	5.46	6.68	10.23	4.77
Heat fluxes					
EM	4.54	-3.62	-2.67	-0.77	2.85
IM	26.34	-7.85	-5.45	2.44	10.29
L	9.71	-4.51	-3.11	0.02	4.53

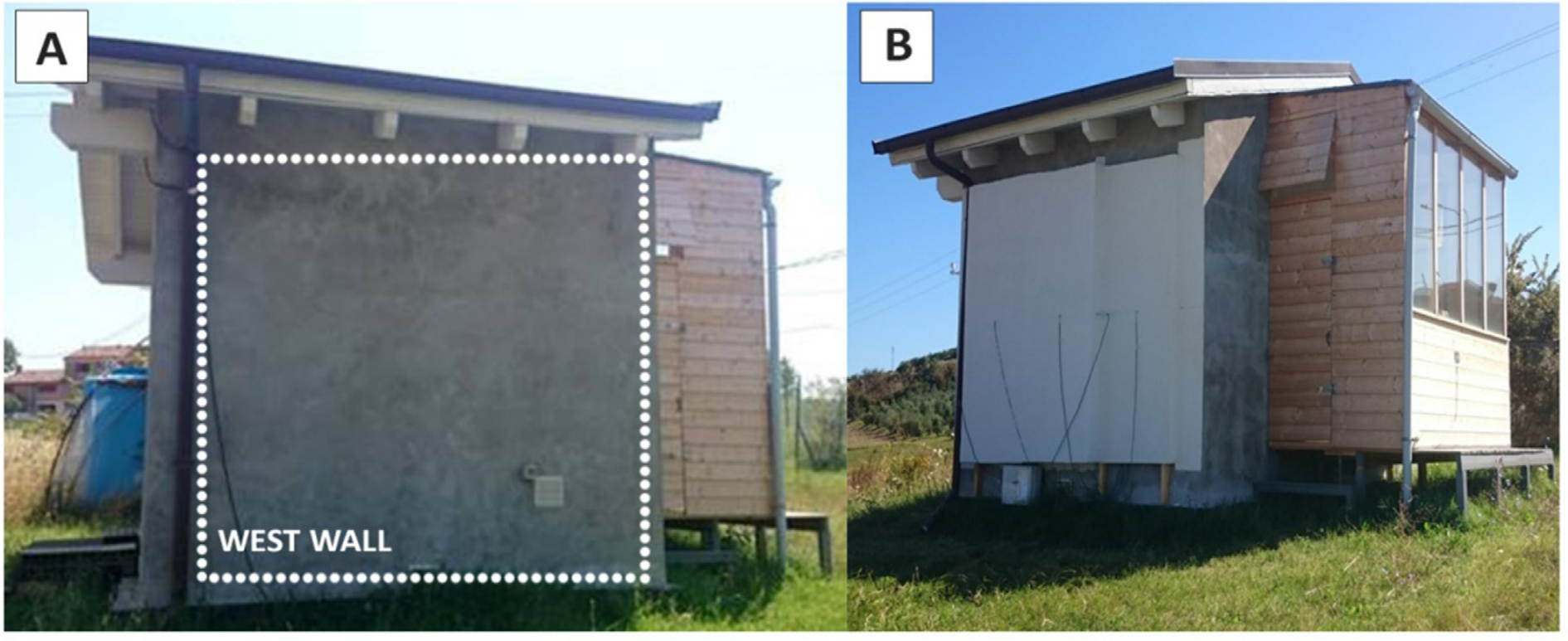
A
WEST WALL
B

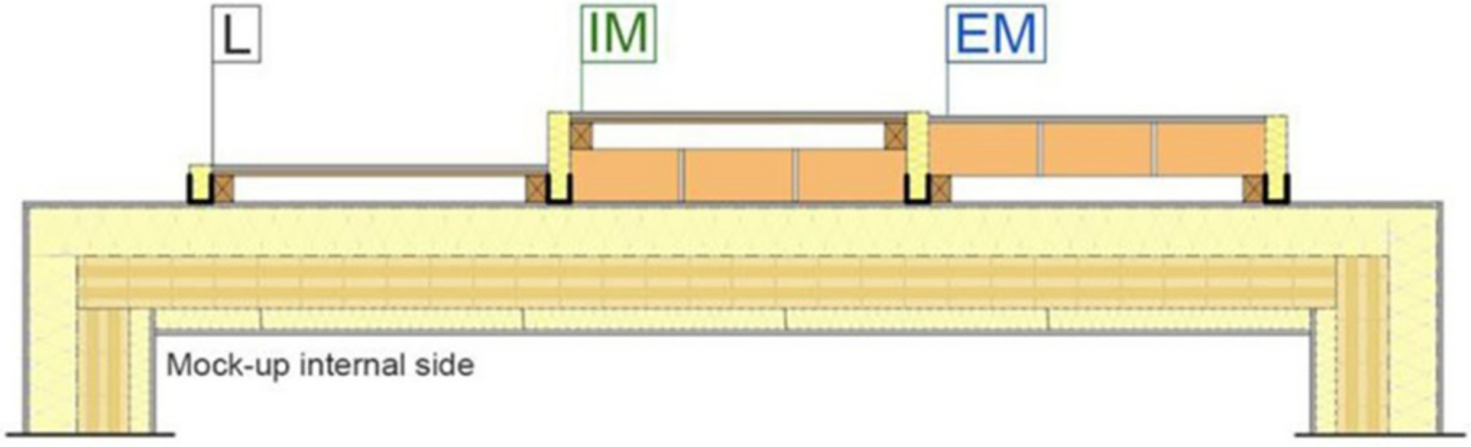

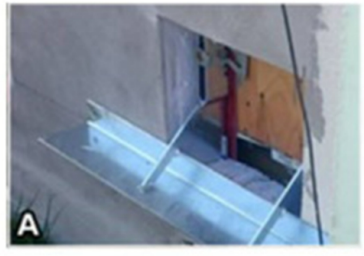

Thermal cutting plate

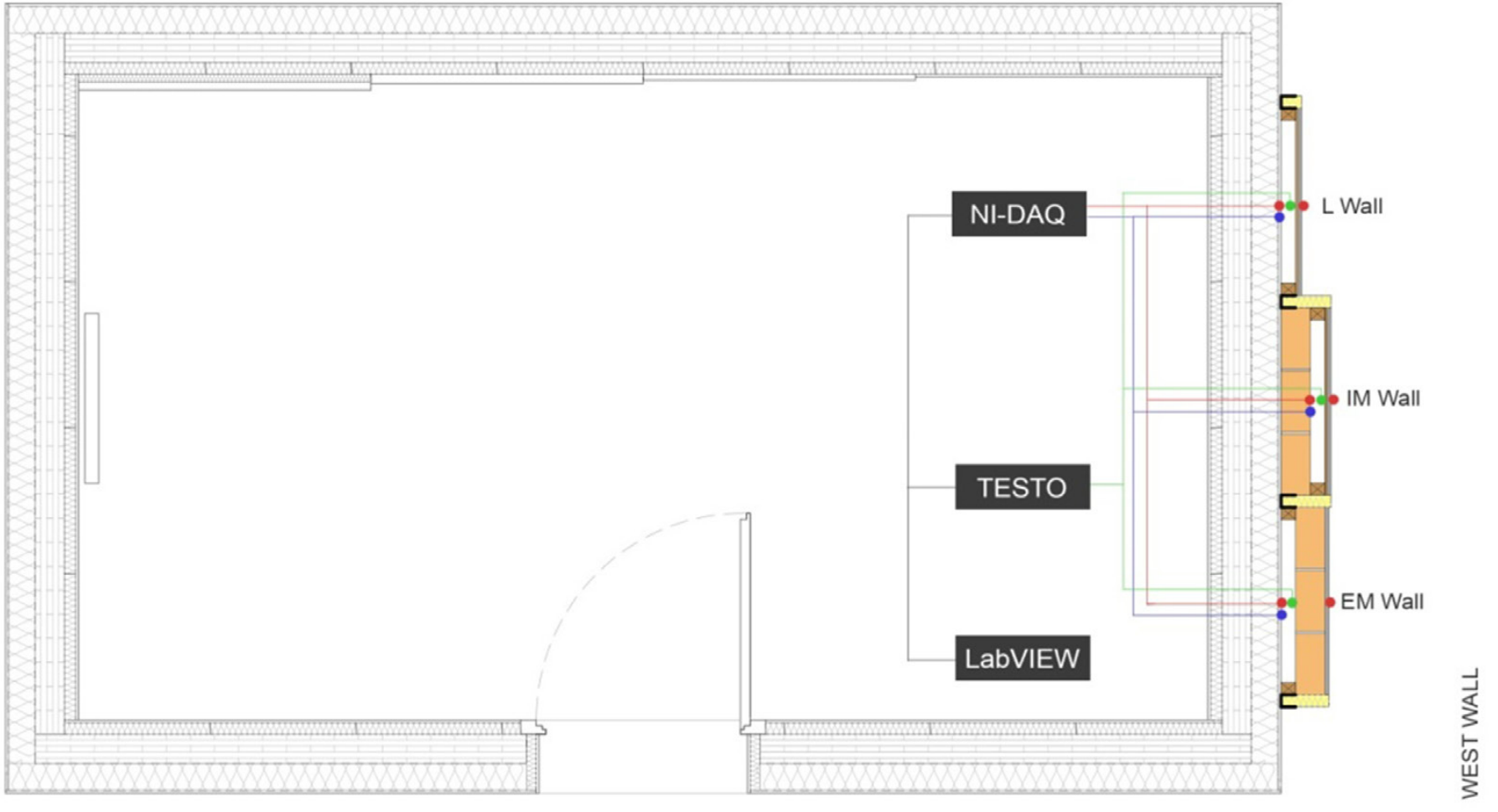

Legend:

- Thermo-resistance sensors on the outer (115 cm) and inner surface (68 cm, 115 cm, 168 cm)
- Heat flux plate (115 cm)
- Anemometer (115 cm)

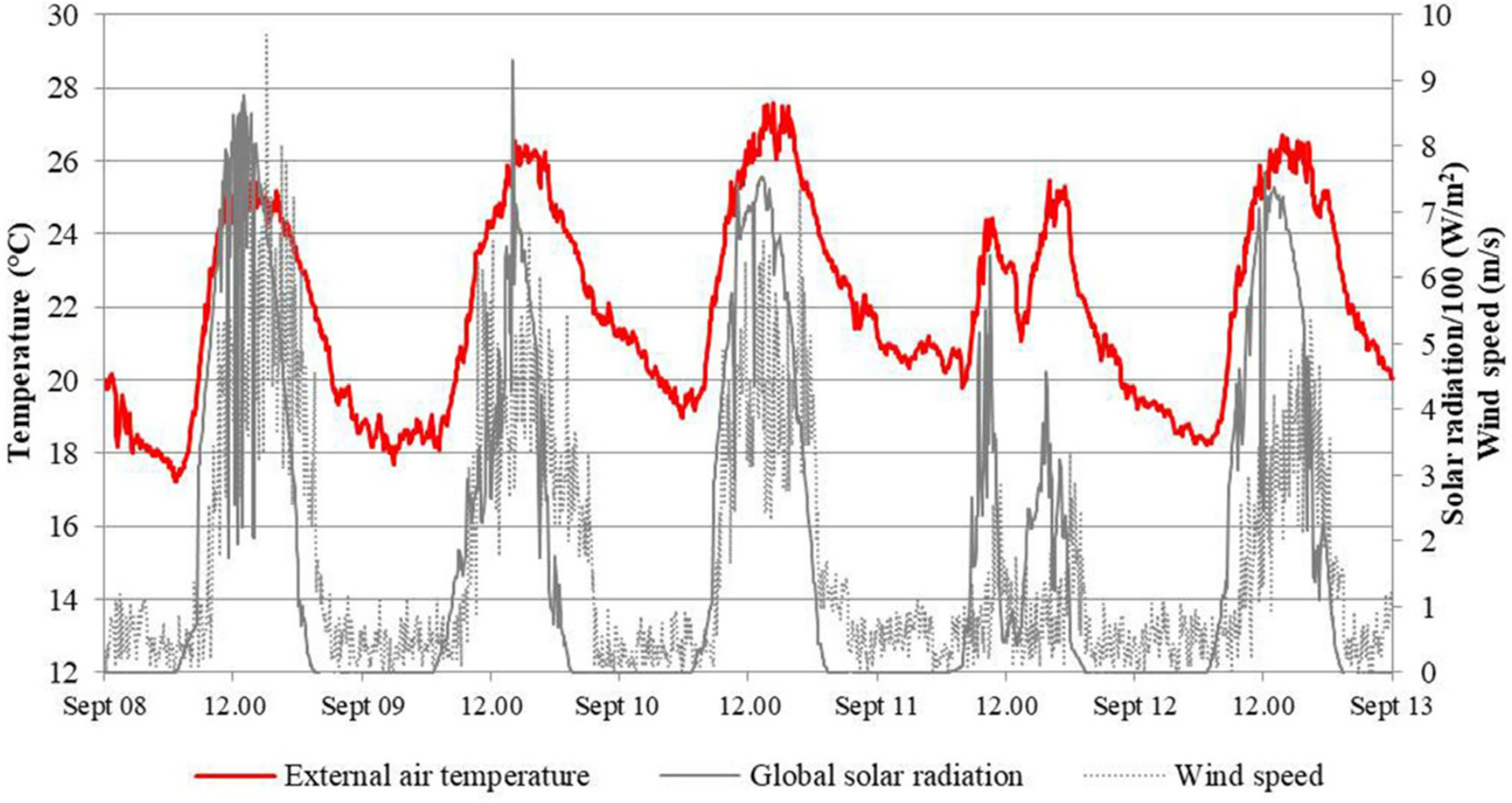
30
28
26
24
22
20
18
16
14
12
Temperature (°C)
10
9
8
7
6
5
4
3
2
1
0
Solar radiation/100 (W/m²)
Wind speed (m/s)
Sept 08
12.00
Sept 09
12.00
Sept 10
12.00
Sept 11
12.00
Sept 12
12.00
Sept 13
External air temperature
Global solar radiation
Wind speed

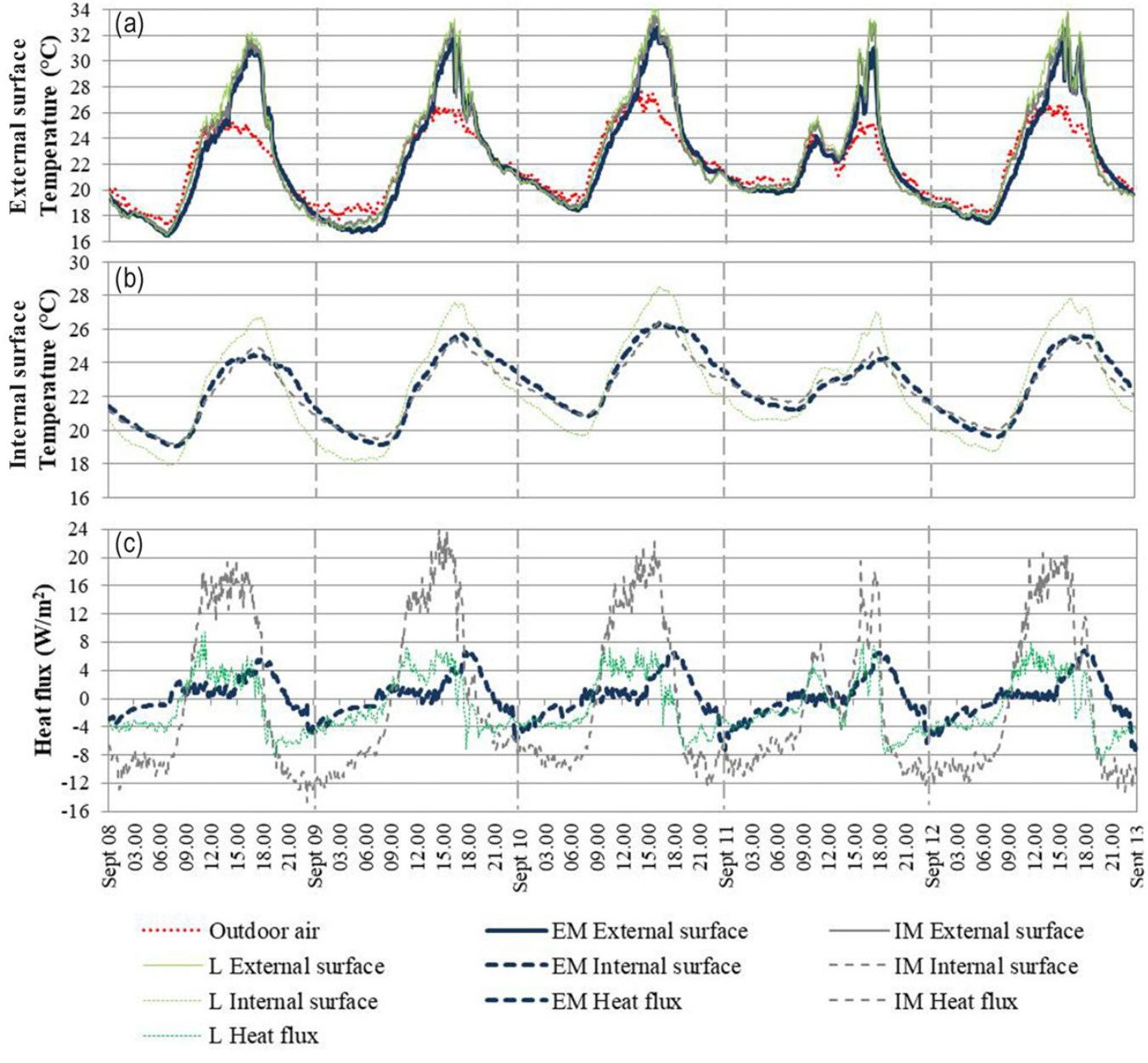
(a)
External surface Temperature (°C)
34
32
30
28
26
24
22
20
18
16
(b)
Internal surface Temperature (°C)
30
28
26
24
22
20
18
16
(c)
Heat flux (W/m²)
24
20
16
12
8
4
0
-4
-8
-12
-16
Sept 08
03.00
06.00
09.00
12.00
15.00
18.00
21.00
Sept 09
Sept 10
Sept 11
Sept 12
Sept 13
Outdoor air
L External surface
L Internal surface
L Heat flux
EM External surface
EM Internal surface
EM Heat flux
IM External surface
IM Internal surface
IM Heat flux

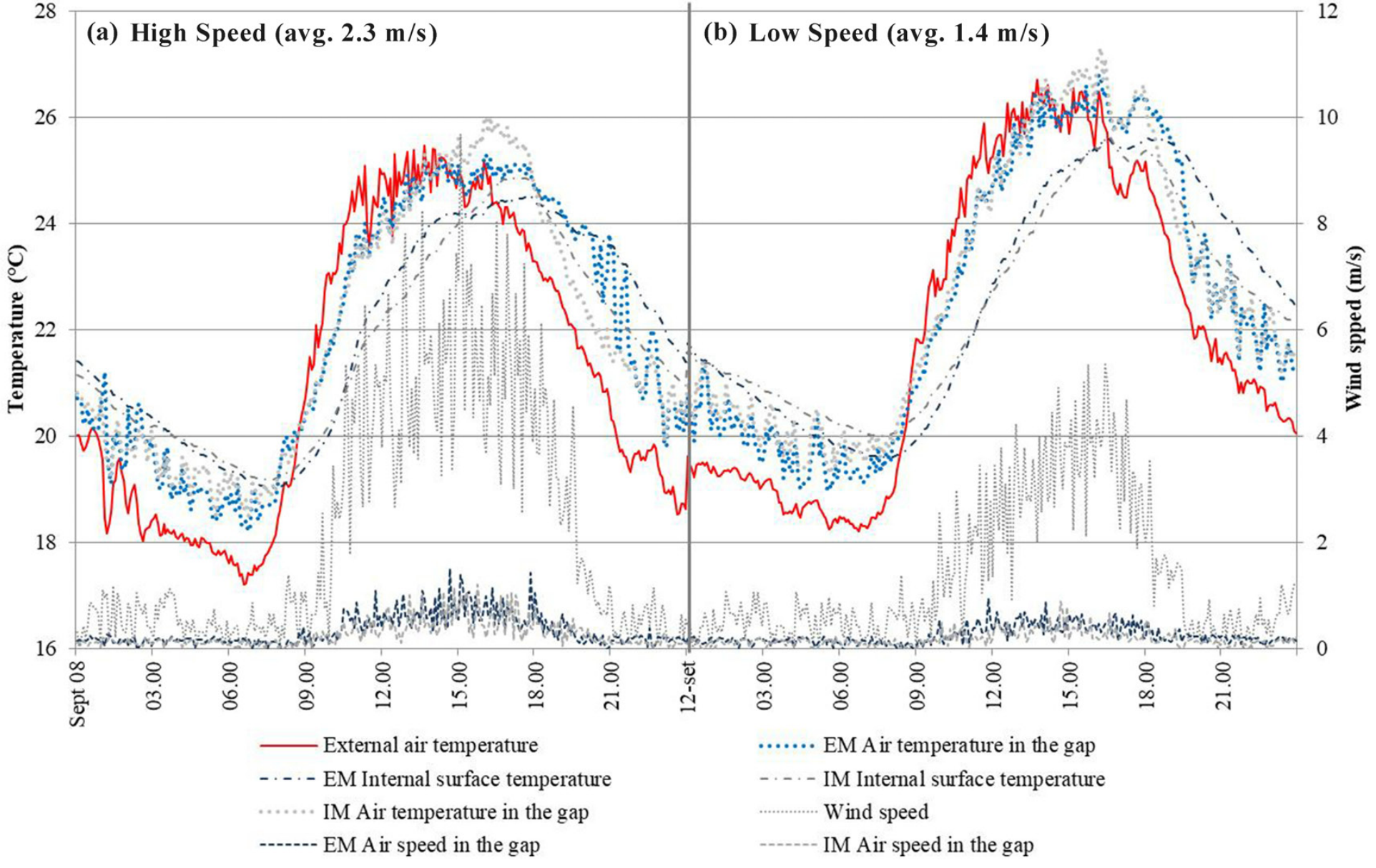
(a) High Speed (avg. 2.3 m/s)
(b) Low Speed (avg. 1.4 m/s)
Temperature (°C)
Wind spped (m/s)
28
26
24
22
20
18
16
12
10
8
6
4
2
0
Sept 08
03.00
06.00
09.00
12.00
15.00
18.00
21.00
12-set
03.00
06.00
09.00
12.00
15.00
18.00
21.00
External air temperature
EM Air temperature in the gap
EM Internal surface temperature
IM Internal surface temperature
IM Air temperature in the gap
Wind speed
EM Air speed in the gap
IM Air speed in the gap

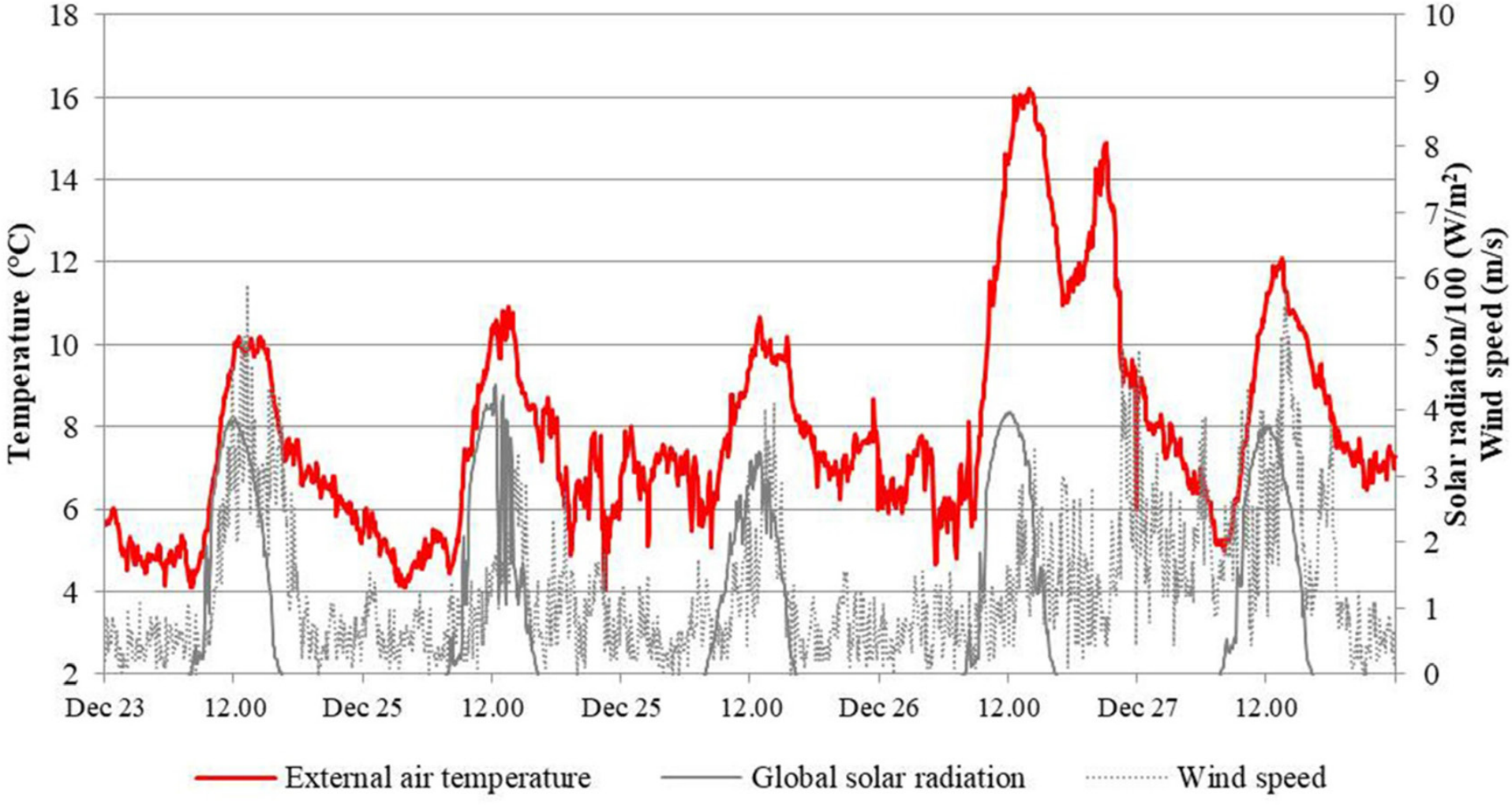
Temperature (°C)
Solar radiation/100 (W/m²)
Wind speed (m/s)
18
16
14
12
10
8
6
4
2
10
9
8
7
6
5
4
3
2
1
0
Dec 23
12.00
Dec 25
12.00
Dec 25
12.00
Dec 26
12.00
Dec 27
12.00
External air temperature
Global solar radiation
Wind speed

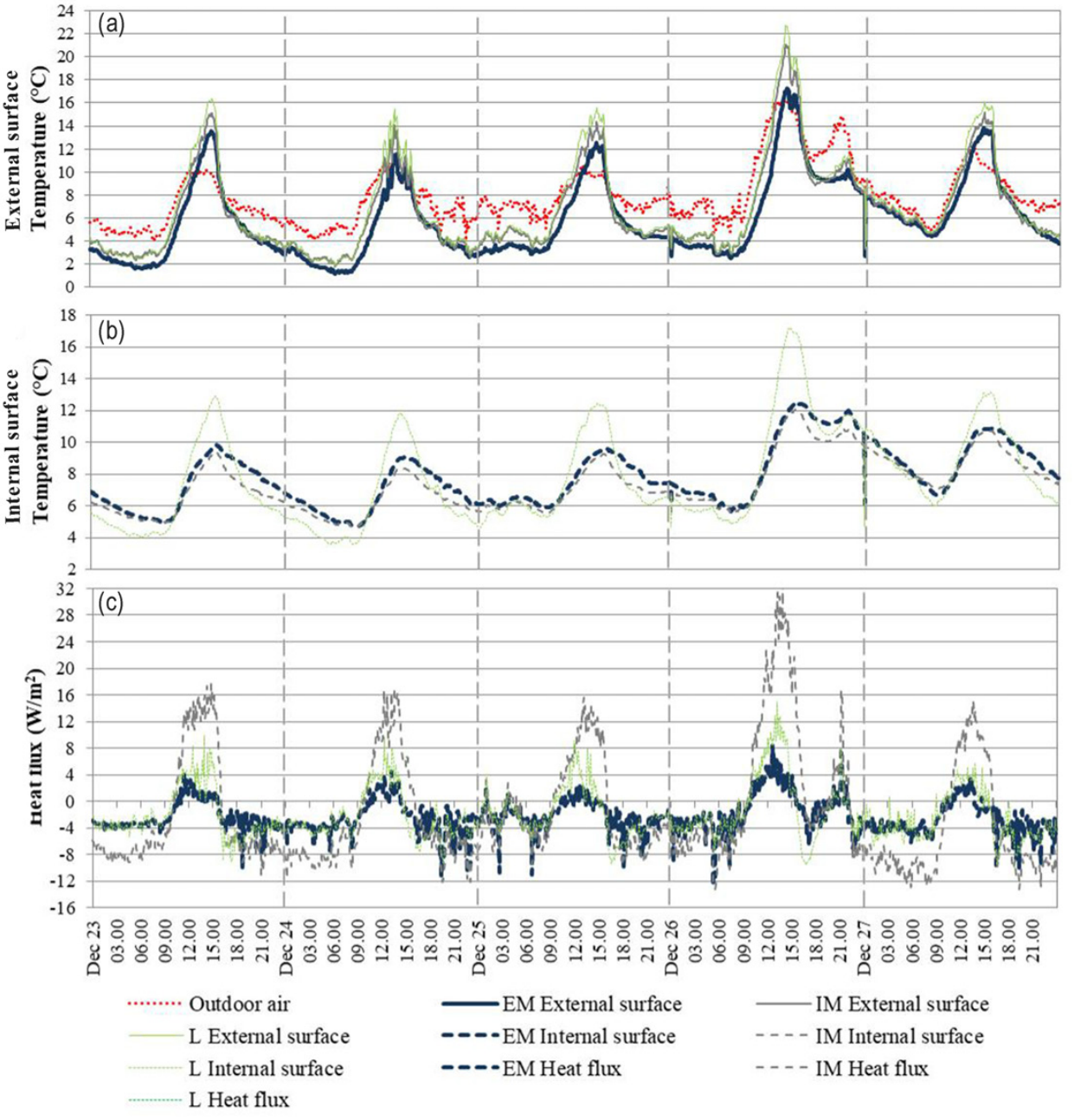
(a)
External surface Temperature (°C)
(b)
Internal surface Temperature (°C)
(c)
Heat flux (W/m²)
Dec 23
Dec 24
Dec 25
Dec 26
Dec 27
Outdoor air
L External surface
L Internal surface
L Heat flux
EM External surface
EM Internal surface
EM Heat flux
IM External surface
IM Internal surface
IM Heat flux

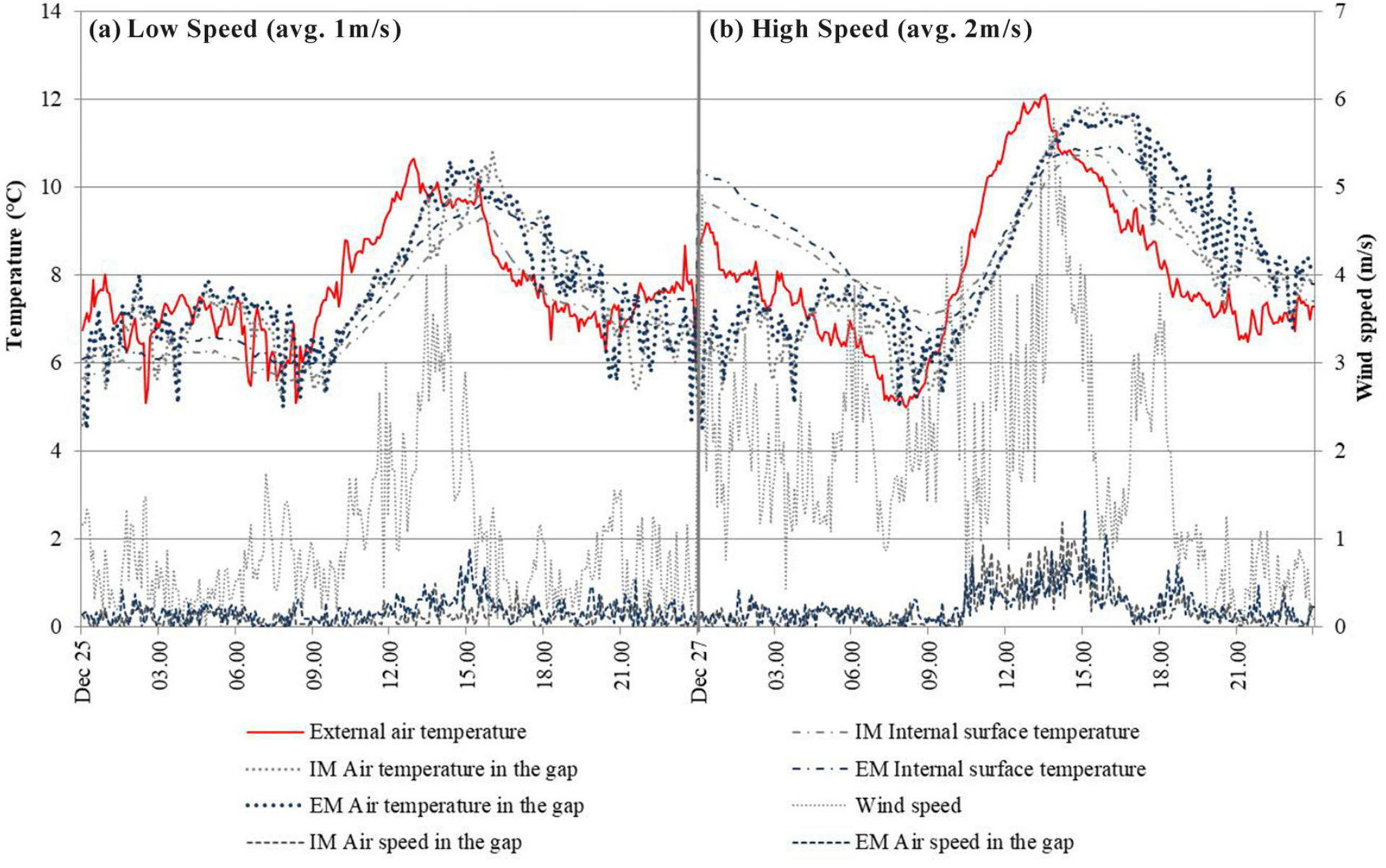
(a) Low Speed (avg. 1m/s)
(b) High Speed (avg. 2m/s)
Temperature (ºC)
Wind spped (m/s)
14
12
10
8
6
4
2
0
7
6
5
4
3
2
1
0
Dec 25
03.00
06.00
09.00
12.00
15.00
18.00
21.00
Dec 27
03.00
06.00
09.00
12.00
15.00
18.00
21.00
External air temperature
IM Air temperature in the gap
EM Air temperature in the gap
IM Air speed in the gap
IM Internal surface temperature
EM Internal surface temperature
Wind speed
EM Air speed in the gap

(a)

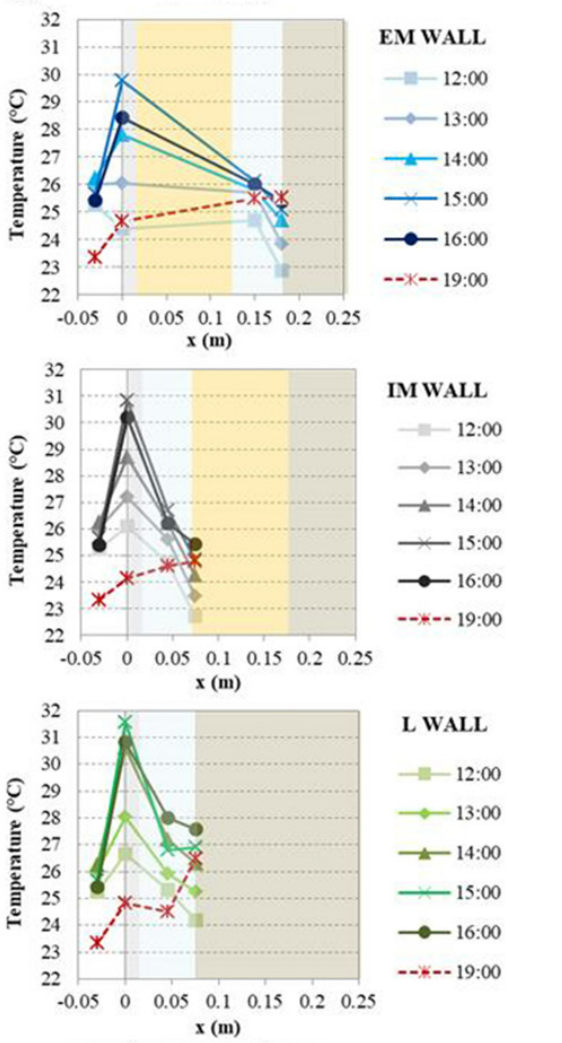

(b)

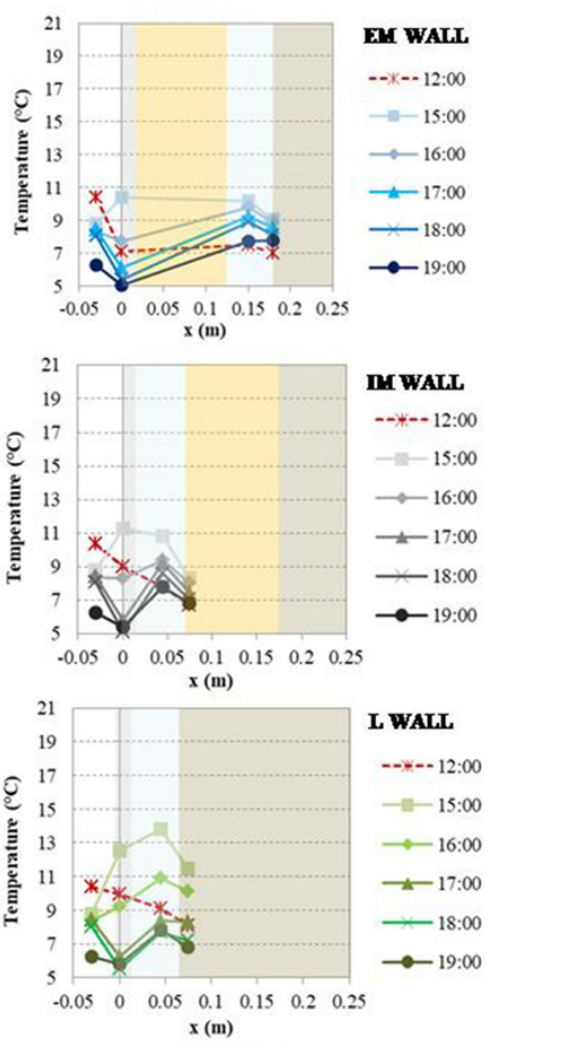

Time (hh:mm)	Solar radiation (W m^{-2})	Wind speed (m s^{-1})	Air gap speed (m/s)		
			EM	IM	L
12:00	298	1.34	0.32	0.18	0.42
13:00	737	3.34	0.57	0.21	0.6
14:00	699	3.67	0.27	0.33	0.35
15:00	613	3.78	0.64	0.16	0.22
16:00	216	3.21	0.47	0.22	0.25
19:00	17	1.48	0.13	0.18	0.19

Time (hh:mm)	Solar radiation (W m^{-2})	Wind speed (m s^{-1})	Air gap speed (m/s)		
			EM	IM	L
12:00	409	1.57	0.29	0.28	0.37
15:00	149	2.33	0.50	0.33	0.72
16:00	16	1.09	0.23	0.23	0.17
17:00	0	0.21	0.19	0.08	0.18
18:00	0	0.44	0.07	0.06	0.2
19:00	0	1.34	0.18	0.05	0.04

Tables

Table 1. Composition of the Ventilated Skin prototypes.

VS with no mass (L)	VS with internal mass (IM)	VS with external mass (EM)
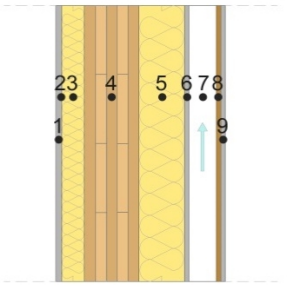	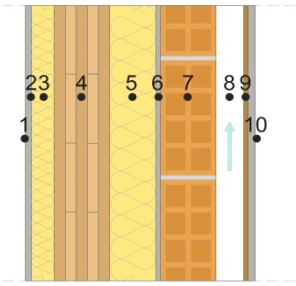	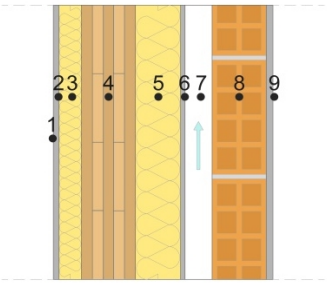
Layer		
1 Internal Plasterboard	Internal Plasterboard	Internal Plasterboard
2 Vapour Barrier	Vapour Barrier	Vapour Barrier
3 Internal Insulation	Internal Insulation	Internal Insulation
4 Cross laminated timber	Cross laminated timber	Cross laminated timber
5 External Insulation	External Insulation	External Insulation
6 Cement mortar	Cement mortar	Cement mortar
7 Air Cavity	Hollow Brick	Air Cavity
8 OSB Panel	Air Cavity	Hollow Brick
9 External Plaster	OSB Panel	External Plaster
10 -	External Plaster	-

Table 2. Thermo-physical properties of the layers.

Material	**Thickness (m)**	**Thermal conductivity (W/mK)**	**Specific heat capacity (J/kgK)**	**Density (kg/m^3)**
Internal Plasterboard	0.0125	0.2	837	760
Vapour Barrier	-	0.17	1500	425
Internal Insulation	0.05	0.035	1030	70
Cross laminated timber	0.12	1.4	2700	500
External Insulation	0.10	0.036	1030	90
Cement mortar	0.015	0.48	1000	1150
Hollow Brick	0.12	0.292	1000	920
Air Cavity*	0.06	-	-	-
External Plaster	0.012	0.33	1110	1150
OSB Panel	0.009	0.1	1700	600

*Thermal resistance of 0.18 m^{2}K/W

Table 3. VSs' steady state and dynamic thermal parameters.

Thermal Properties	Wall Typology		
	L	**IM**	**EM**
Thermal Transmittance U (W/m^2K) [a, b]	0.22	0.20	0.22
Decrement Factor f^b	0.08	0.04	0.08
Time Lag Δt (h) [b]	8.4	13.9	8.4
Periodic Thermal Trasmittance Y_{12} (W/m^2K) [b]	0.017	0.07	0.017
External Areal Heat Capacity k_2 (kJ/m^2K) [c]	28	40	60

[a] calculated according to EN ISO 6946:2008.
U < 0.26 Wm^2/K according to the Italian regulation on energy efficiency (D.M. 2015).

[b] calculated according to EN ISO 13786:2008, considering a well-ventilated facade by disregarding the outer layer.

[c] calculated according to EN ISO 13786:2008, considering all the envelope layers and still air in the gap to better highlight the role of the external mass.

Table 4. 99th percentile, median and interquartile range (IQR) of the surface temperatures and the heat fluxes during the representative summer period.

	99 Percentile	**Q1**	**Q2**	**Q3**	**IQR**
External surface temperature					
EM	31.74	19.03	21.33	24.79	5.76
IM	32.86	19.11	21.18	25.40	6.29
L	33.29	19.00	21.27	25.92	6.92
Internal surface temperature					
EM	26.19	21.00	22.70	24.18	3.18
IM	26.30	20.99	22.39	23.79	2.81
L	28.21	19.96	22.02	24.81	4.85
Heat fluxes					
EM	6.44	-1.54	0.13	1.58	3.12
IM	21.14	-9.18	-6.08	9.21	18.40
L	6.96	-4.00	-2.62	2.85	6.86

Table 5. 99th percentile, median and interquartile range (IQR) of the surface temperatures and the heat fluxes during the representative winter period.

	99 Percentile	**Q1**	**Q2**	**Q3**	**IQR**
External surface temperature					
EM	16.09	3.29	4.89	8.11	4.82
IM	18.73	4.02	5.16	8.75	4.73
L	19.96	4.14	5.44	9.42	5.28
Internal surface temperature					
EM	12.36	6.29	7.48	9.18	2.89
IM	11.89	5.93	7.02	8.49	2.56
L	16.84	5.46	6.68	10.23	4.77
Heat fluxes					
EM	4.54	-3.62	-2.67	-0.77	2.85
IM	26.34	-7.85	-5.45	2.44	10.29
L	9.71	-4.51	-3.11	0.02	4.53

AUTHOR DECLARATION

We wish to confirm that there are no known conflicts of interest associated with this publication and there has been no significant financial support for this work that could have influenced its outcome.

We confirm that the manuscript has been read and approved by all named authors and that there are no other persons who satisfied the criteria for authorship but are not listed. We further confirm that the order of authors listed in the manuscript has been approved by all of us.

We confirm that we have given due consideration to the protection of intellectual property associated with this work and that there are no impediments to publication, including the timing of publication, with respect to intellectual property. In so doing we confirm that we have followed the regulations of our institutions concerning intellectual property.

We understand that the Corresponding Author is the sole contact for the Editorial process (including Editorial Manager and direct communications with the office). He/she is responsible for communicating with the other authors about progress, submissions of revisions and final approval of proofs. We confirm that we have provided a current, correct email address which is accessible by the Corresponding Author and which has been configured to accept email from:

Francesca Stazi

E-mail: f.stazi@univpm.it

Signed by all authors as follows:

Giulia Ulpiani

Marianna Pergolini

Costanzo Di Perna

Marco D'Orazio

CRediT Author statement

Francesca Stazi (corresponding auhor)**:** Resources, Conceptualization, Methodology Reviewing, Writing - Review & Editing.

Giulia Ulpiani: Software, Data curation, Writing - Review & Editing.

Marianna Pergolini: Data curation, Writing - Original Draft, Visualization.

Costanzo Di Perna: Supervision, Resources, Software.

Marco D'Orazio: Supervision.